

Document Version

Final published version

Licence

CC BY

Citation (APA)

Veeger, M. I. A., Ottele, M., & Jonkers, H. M. (2026). How moss affects urban temperatures: The effects of moss on the thermal dynamics of an urban cementitious surface. *Science of the Total Environment*, 1034, Article 181830. <https://doi.org/10.1016/j.scitotenv.2026.181830>

Important note

To cite this publication, please use the final published version (if applicable). Please check the document version above.

Copyright

In case the licence states “Dutch Copyright Act (Article 25fa)”, this publication was made available Green Open Access via the TU Delft Institutional Repository pursuant to Dutch Copyright Act (Article 25fa, the Taverne amendment). This provision does not affect copyright ownership. Unless copyright is transferred by contract or statute, it remains with the copyright holder.

Sharing and reuse

Other than for strictly personal use, it is not permitted to download, forward or distribute the text or part of it, without the consent of the author(s) and/or copyright holder(s), unless the work is under an open content license such as Creative Commons.

Takedown policy

Please contact us and provide details if you believe this document breaches copyrights. We will remove access to the work immediately and investigate your claim.



How moss affects urban temperatures: The effects of moss on the thermal dynamics of an urban cementitious surface

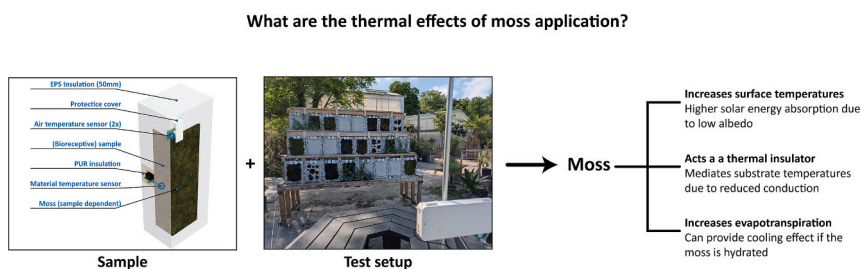
M. Veeger^{a,*}, M. Ottel  ^a, H.M. Jonkers^a

^a Delft University of Technology, Faculty of Civil Engineering and Geosciences, Department of Materials, Mechanics, Management & Design (3Md), Materials and Environment, Stevinweg 1, 2628, CN, Delft, Netherlands

HIGHLIGHTS

- The effects of moss on air, surface, and substrate temperatures were tested.
- Moss application increased air and surface temperatures under direct sunlight.
- Moss acted as a thermal insulator, reducing heat flux to and from the substrate.
- Moss can reduce temperatures through evaporative cooling when hydrated.

GRAPHICAL ABSTRACT



ARTICLE INFO

Keywords:

Moss
Bioreceptive concrete
Heat balance
Temperature
City

ABSTRACT

Urban surfaces often exhibit higher temperatures than natural ones, increasing heat stress in urban inhabitants. Plants can provide a solution due to their cooling effect. Whereas this has been investigated in vascular plants, this study is the first to investigate the influence of three moss species (*Grimmia pulvinata*, *Ptychostomum capillare*, and *Brachythecium rutabulum*) attached to a cementitious surface on air, surface, and substrate temperatures. They were compared to bare mortar, mortar covered with the climbing plant *Hedera helix*, and a moss-climber combination under varying weather conditions. Moss was found to affect temperatures in three ways. Firstly, moss increased surface temperatures in direct sunlight, with an average daytime increase of +1.5 °C to +4.1 °C compared to bare mortar. Secondly, moss exhibited insulating properties, dampening the heat flux to and from the underlying substrate. This reduced heat transfer to the substrate during warm days, limiting heat gain, but also reduced heat transfer from the substrate at night, leading to average nighttime temperatures inside the substrate that were higher (+3.0 °C to +3.8 °C) than in the bare samples. Finally, when moss was hydrated, an evaporative cooling effect could be observed, but it lasted only a few hours after watering. These findings suggest that moss could be a net positive in colder seasons or climates, but that under warmer conditions, it is best to keep moss hydrated or shaded during sun-exposed periods. Therefore, a moss-climber combination appears promising, combining the thermal insulation, acoustic and air-quality benefits of moss with the shading effect of climbing plants.

* Corresponding author.

E-mail address: m.i.a.veeger@tudelft.nl (M. Veeger).

1. Introduction

Global surface temperatures have been rising due to human-caused climate change. The overall average surface temperature in 2011–2020 is estimated to be 1.09 °C higher than in 1850–1900, and the average surface temperature over land is estimated to be 1.59 °C higher (IPCC, 2023a). Furthermore, the current estimation is that with current climate policies, this will increase to a 2.2 to 3.5 °C rise in temperature by 2100 (IPCC, 2023b). This rise in temperature, in turn, leads to increased negative health outcomes, including heat stroke, cardiovascular disease, mental health issues and adverse birth outcomes (Liu et al., 2022; Liu et al., 2021; Ebi et al., 2021; Zhang et al., 2017). These issues are particularly prominent in cities, where the so-called Urban Heat Island (UHI; the phenomenon where the temperature in cities is higher than in the surrounding area) effect exacerbates heat-related health risks (Heaviside et al., 2017). Typically, the difference in temperature between urban and rural areas is in the order of a few degrees, but can reach 10–15 °C in extreme cases (Mentaschi et al., 2022). A variety of factors contribute to this dissimilarity, including the different properties of the materials used in urban surfaces compared to natural areas (Oke et al., 1991). This change in thermal properties, in turn, affects the urban energy balance (Fig. 1). This leads to an increased sensible heat flux [Q_h] and outgoing longwave radiation [$L\uparrow$], causing higher heat stress experienced by urban inhabitants (Havenith and Fiala, 2015; Asaeda et al., 1996; Takebayashi and Moriyama, 2012).

First of all, compared to more natural, rural surroundings, urban materials generally have lower albedo (α) values, meaning they absorb a higher portion of incoming solar radiation rather than reflecting it (Trlica et al., 2017; Hou et al., 2014; Jin et al., 2005). Second, as both vegetation coverage and soil water storage are often minimal in urban areas, evapotranspiration [E], and thus latent heat dissipation [Q_E] is greatly reduced (Oke, 1987; Wang et al., 2020; Taha, 1997). Finally, the high heat storage capacity of urban surface materials can initially

decrease temperatures in the city during the day. As heat energy is stored in the material [ΔQ_S], some of the daytime Urban Heat Island is mitigated. The release of this energy during the night, however, can lead to higher temperatures during the nighttime instead (Kusaka and Kimura, 2004; Nunez and Oke, 1977) thereby contributing to the Urban Heat Island (UHI) effect.

One well-researched strategy for cooling cities is by adding vegetation, either through solitary trees, green areas, or vertical and horizontal green structures, with substantial scientific research available showing that plants can decrease land surface temperatures and the extent of the urban heat island [e.g. (Kumar and Shekhar, 2015), (Tamaskani Esfehankalateh et al., 2021; Al-Saadi et al., 2020; Zhao et al., 2020; Yan et al., 2020; Duncan et al., 2019; Ossola et al., 2021; Edmondson et al., 2016; Millward et al., 2014; Davis et al., 2016; Susca et al., 2011; Weng et al., 2004; Gallo et al., 1993; Feyisa et al., 2014)]. Plants can affect urban surface temperatures, and thereby air and mean radiant temperatures, through four primary mechanisms (Pérez et al., 2011):

1. shading (reduced incoming shortwave radiation [$K\downarrow$]).
2. insulation (reduced conduction [Q_G] and thermal diffusion [h]).
3. evaporative cooling (increased latent heat flux [Q_E]).
4. wind blockage (reduced sensible heat flux [Q_H]).

However, research on the urban cooling potential of plants has so far been focused on vascular plants (or tracheophytes). With recent developments in bioreceptive concrete, a concrete typology that allows biological materials – such as mosses – to grow directly on its surface, acting as a growing substrate (Stohl et al., 2023), the question arises whether this cooling potential also extends to other plants, specifically mosses. Mosses in the built environment have already been linked to increased acoustic and particulate matter absorption compared to other plants (Veeger et al., 2025a; Perini et al., 2025), and research on moss-containing biocrusts in natural ecosystems has shown that moss can both

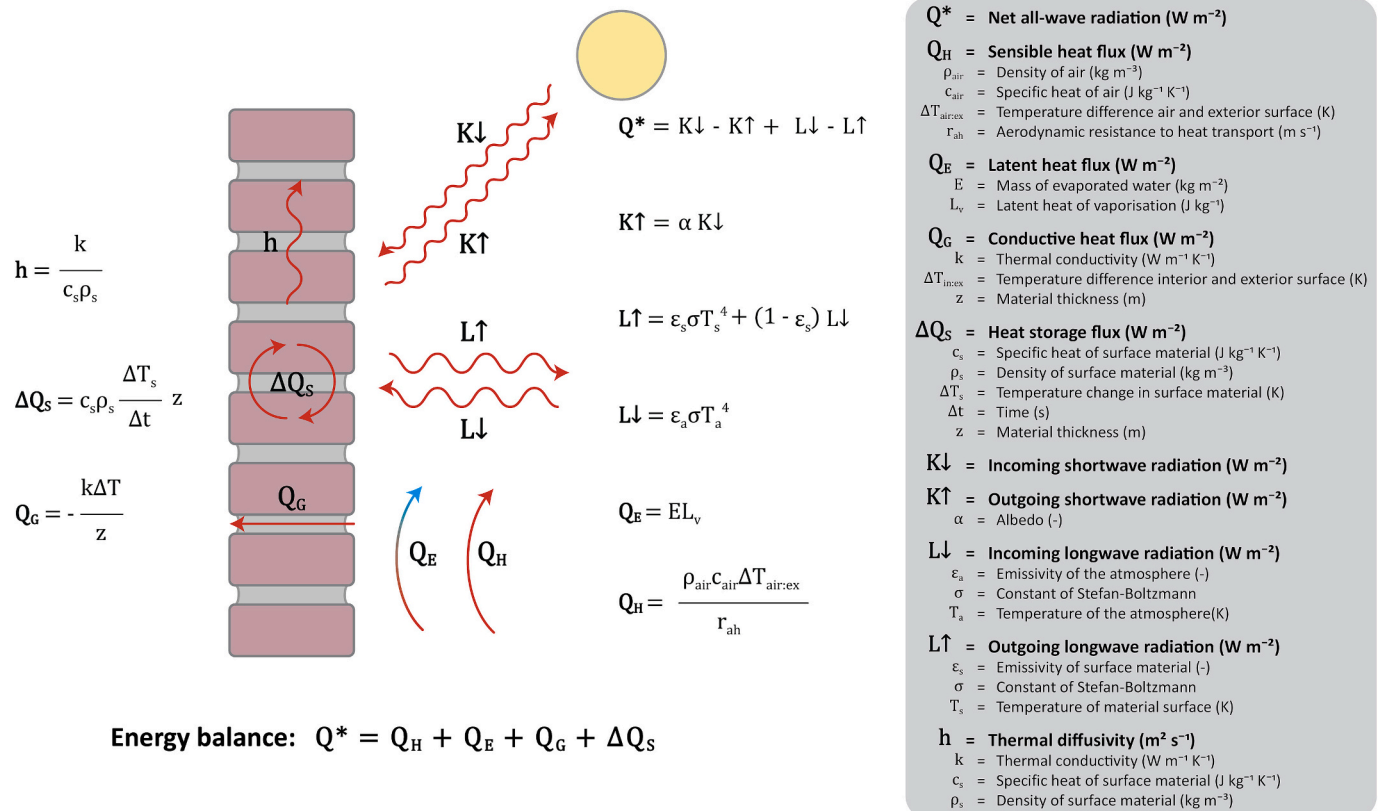


Fig. 1. Overview of the energy balance and heat fluxes of an (urban) surface material. Based on Oke (Oke, 1987) and Allen, et al. (Allen et al., 2002).

decrease and increase soil and surface temperatures compared to bare soil, depending on several factors, such as species, moisture availability, season, and time of day, through a combination of altering surface albedo, evapotranspiration and insulation [e.g. (Xiao and Bowker, 2020), (Xiao et al., 2016; Xiao et al., 2019; Soudzilovskaia et al., 2013; Li and Xiao, 2022; Liu et al., 2006; Zhang et al., 2009)]. However, research on the effect of moss on temperatures in the urban environment is very limited. Of the research that is available, Amir, et al. (Amir et al., 2018) found that a Sunagoke moss sheet-based green roof system yielded lower surface and internal temperatures than a conventional roof in a laboratory setting. Similarly, Perini, et al. (Perini et al., 2022) found that their moss-based façade system, consisting of moss grown on a textile surface in combination with an irrigation system, decreased surface temperatures compared to surrounding masonry walls and an unidentified roofing system under exterior conditions. Finally, Jongsoo and Jeasun (Jongsoo and Jeasun, 2026) found that a roof covered with irrigated moss panels could lower both surface and indoor temperatures. However, in none of this research did the moss grow directly on the building material (as is the case with bioreceptive building materials), nor was it compared to a bare cementitious surface, the most commonly used building material worldwide (Monteiro et al., 2017).

This research aimed to investigate the effects of moss growth on bioreceptive mortar and its influence on the thermal properties of this mortar layer through a comparative field experiment. Based on the existing literature, the following experimental hypotheses were formulated about the effect of moss application on the thermal dynamics of a cementitious surface:

1. An increase in surface, material and local air temperature under sunlight

As the albedo of moss (0.07) has been found to be lower than that of concrete (0.13) (Stache et al., 2022), a smaller fraction of incoming solar radiation should get reflected ($K\uparrow$), which means this energy instead gets converted into heat energy on the moss surface. This, in turn, increases the conductive (Q_G) and sensible (Q_H) heat flux, leading to increased underlying material and local air temperatures, respectively, as well as an increase in outgoing longwave radiation ($L\uparrow$).

2. Reduced temperature fluctuations in the underlying material

The thermal conductivity of moss (0.03 to 0.6 W m⁻¹ K⁻¹) (O'Donnell et al., 2009a; Sharratt, 1997; Hinzman et al., 1991), is significantly lower than that of mortar (1.5 to 2.7 W m⁻¹ K⁻¹) (Shafiqh et al., 2020). This leads to a reduced conductive (Q_G) heat flux, which means that the temperature inside the underlying material should be more stable.

3. A decrease in surface, material and local air temperature under hydrated conditions

Moss can hold on to several times their own body weight in water (Gimingham and Smith, 1971), which means there is high potential for a latent heat flux due to evapotranspiration when the moss is hydrated. This, in turn, should reduce the surface temperature and thus the conductive (Q_G), sensible (Q_H) and outgoing longwave radiation fluxes ($L\uparrow$), leading to lower overall temperatures.

2. Methodology

2.1. Sample preparation

For the purposes of this research, a total of 24 mortar samples were prepared, with 3 samples per treatment (Table 2), each measuring 300x200x60 mm. Of these mortar samples, 21 were produced using a bioreceptive mortar mixture (Veeger et al., 2021) and 3 using a reference mortar mixture (Table 1).

During casting, two temperature sensors (one primary and one backup) were embedded at a depth of 30 mm in each concrete sample (see Paragraph 2.3). Samples were demoulded after two days and then

Table 1

Mix designs of the two mortar mixtures used.

Constituents	Bioreceptive mixture	Reference mixture
Binder: CEMIII/B	250 kg m ⁻³	450 kg m ⁻³
Water	262 kg m ⁻³	225 kg m ⁻³
Aggregate: Recycled concrete (0-4 mm)	1460 kg m ⁻³	
Aggregate: River sand (0-4 mm)		1350 kg m ⁻³
Additive: Bone ash	12.5 kg m ⁻³	

cured at 20 degrees Celsius in dry conditions and with twice-weekly surface wetting for four weeks. After the curing period, the samples were insulated with 50 mm thick EPS foam on all sides except the front-facing surface to minimise heat exchange through these sides (Fig. 2). An opening was left in the insulation on the back side to allow connection of the temperature sensor cables. Once the sensors were connected, this opening was sealed with PUR foam. As part of this experiment, three moss species were tested on the bioreceptive mortar samples along with one climbing plant species:

- *Grimmia pulvinata* (Hedw.) Sm. [*G. pulvinata*], an acrocarp species which is a very common cosmopolitan coloniser of cementitious surfaces (Veeger et al., 2025b)
- *Brachythecium rutabulum* (Hedw.) Schimp. [*B. rutabulum*], a pleurocarp species that has already been successfully cultivated on bioreceptive concrete (Veeger et al., 2026).
- *Ptychostomum capillare* (Hedw.) Holyoak & N. Pedersen [*P. capillare*], an acrocarp species that has already been successfully cultivated on bioreceptive concrete (Veeger et al., 2026).
- *Hedera helix* L. [*H. helix*], a climbing plant species commonly used in urban greening for its shading potential and adaptability to vertical surfaces.

Normally, the moss is grown on the surface from dried fragments as described in (Veeger et al., 2026). However, as this process can take several months or years to result in mature moss colonies, for those samples which had a moss covering, moss of the respective species was instead harvested from an existing cementitious structure and applied to the mortar surface using a few drops of cyanoacrylate glue (Table 2). Finally, two air temperature sensors were affixed just above each sample using 3M 4496 foam tape and covered with a 3D-printed cover to protect the sensors from the direct influence of rain and sunlight (Fig. 2).

2.2. Sensors and measurements

For the purpose of this research, two custom temperature sensor PCBs were designed. The first is a temperature sensor PCB designed to measure the temperature inside the mortar substrate, built around the Texas Instruments TMP117 IC. This is a low-power digital chip that communicates through the I2C protocol and offers a typical accuracy of ±0.1 °C across its full operating range (−55 °C to 150 °C). Two of these temperature sensors (one primary and one backup) were embedded into the concrete samples during casting, positioned halfway through the sample at a depth of 30 mm (Fig. 2). After curing the concrete samples, sensor accuracy was verified by placing the samples in a temperature-controlled room until thermal equilibrium was reached, after which the sensor readings were cross-referenced. The second custom temperature sensor PCB was an air temperature sensor built around the Texas Instruments HDC3022 IC. This low-power digital chip also communicates via the I2C protocol and provides a typical accuracy of ±0.1 °C across its operating range (−40 °C to 125 °C). It is equipped with a factory-installed IP67 cover for environmental protection. Two of these sensors were placed level to the upper edge of each sample, at a distance of roughly 5 mm from the surface, and covered using a 3D-printed cover to protect the sensor from direct rain and sunlight (Fig. 2). Similar to the

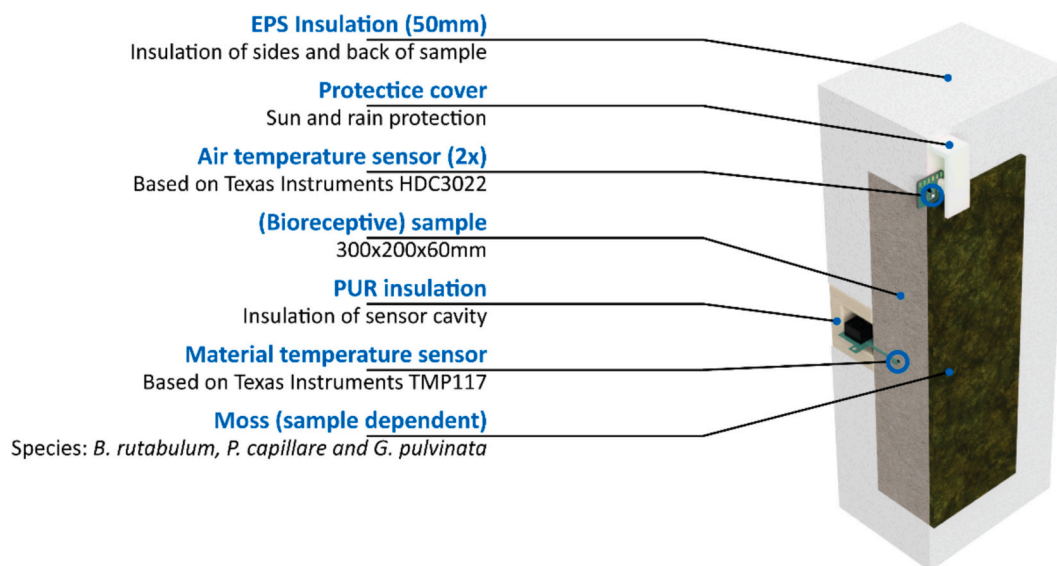


Fig. 2. Section view of an individual sample showing its sensor locations.

Table 2
Overview of all sample treatments.

Sample	Concrete mixture	Vegetation cover
BioRef1 – BioRef 3	Bioreceptive	None
Ref1 - Ref3	Reference	None
HH1 – HH3	Bioreceptive	<i>Hedera helix</i>
HH + GP1 – HH + GP3	Bioreceptive	<i>Hedera helix</i> and <i>Grimmia pulvinata</i>
GP1 – GP3	Bioreceptive	<i>Grimmia pulvinata</i> (100% cover)
GPP01 – GPP3	Bioreceptive	<i>Grimmia pulvinata</i> (~50% cover)
BC1 – BC3	Bioreceptive	<i>Ptychostomum capillare</i> (100% cover)
BR1 – BR3	Bioreceptive	<i>Brachythecium rutabulum</i> (100% cover)

TMP sensors, the accuracy of the sensors was validated in a climate-controlled room.

The third sensor type used was the Adafruit VEML7700, which implements Vishay VEML7700 digital light sensor with a 0–140,000 lx measurement range and a resolution of 0.0336 lx. Although this sensor is limited to the visible light spectrum, it was used to indicate when sunlight was striking the samples and to provide a relative measure of its intensity. Two of these sensors were installed on the test setup, positioned between the samples (Fig. 4). All digital sensors were connected to a custom datalogger built around the Espressif ESP32-S2 microcontroller, which supported up to 4 sensors of each type. Each pair of sensors from a sample was connected to a different datalogger to ensure redundancy. Data was logged every 10 min and stored both locally on an SD card and online in the Arduino CC cloud. Full schematics of the sensors and the data logger used are provided in Fig. 3.

Finally, a CAT S62 Pro smartphone was positioned 3 m from the sample surface to measure outgoing longwave radiation. This smartphone model has a built-in FLIR Lepton 3.5 sensor, capable of detecting longwave infrared radiation in the 8–14 μm range, with a resolution of 160×120 pixels and thermal sensitivity below 50 mK. Images were captured every 10 min using an automated script.

2.3. Test location

Testing took place from February 2025 to June 2025 at the Hortus Botanicus of the TU Delft, located in Delft, the Netherlands. The climate in the Netherlands is temperate oceanic, classified as *Cfb* in the Köppen-Geiger classification system.

To hold all test samples and the sensors, a wooden frame was constructed and positioned facing East in an unshaded area of the Hortus Botanicus (Fig. 4). This orientation was chosen as, although a Southern orientation receives a higher solar radiation budget, not all moss species (in particular the pleurocarp species such as *B. rutabulum*) tolerate these conditions well (Veeger et al., 2026). In this regard, the Eastern aspect receives less solar radiation than the Southern aspect, yet still delivers sufficient shortwave radiation to significantly heat the surface without excessively stressing the moss plants.

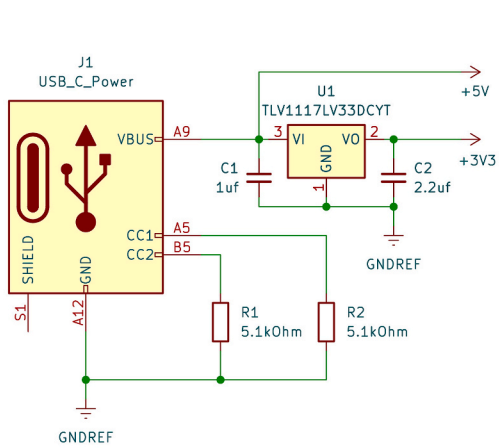
Samples were placed on three different platforms, arranged in a staircase pattern to minimise cross-platform interference. Each platform held eight samples, one of each treatment in a randomised pattern, but ensuring a similar average distance to the middle of the platform for each treatment. Dataloggers were placed behind the samples in a covered space. Two additional air temperature sensors were placed on the Northern aspect of the wooden frame to measure local ambient air temperature, and the light sensors were placed between the samples on the second platform. Finally, the FLIR Lepton infrared camera was placed in a 3D-printed housing at a distance of 3 m from the samples to ensure all samples were in frame simultaneously. Daily precipitation data were collected locally at the Hortus Botanicus, and this data was used for this research.

2.4. Data selection and analysis

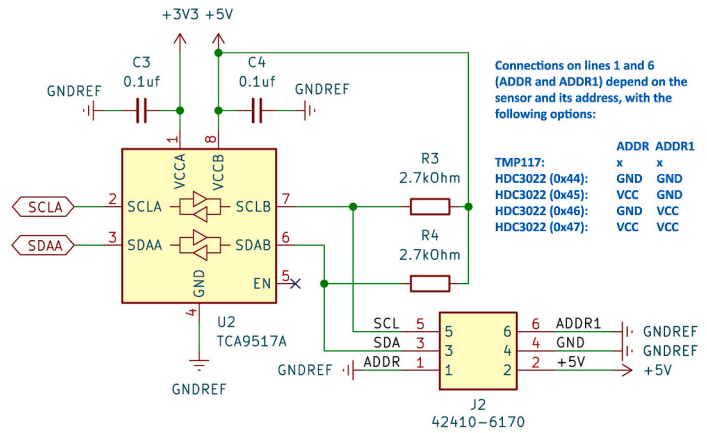
Based on the weather conditions during the testing period, four different 4-day periods with distinct yet relatively stable conditions were selected to best test the three hypothesised thermal dynamics under warm and cold conditions. These were:

- A period of cold weather: ‘**Cold**’. This period was selected to test the insulating effect of moss under cold weather conditions, as well as to determine the solar heat gain and insulating effect under winter conditions.
 - o 17th of February until 20th of February
 - o Average daytime temperature: 4.9 °C; average nighttime temperature: 2.2 °C
- A period of mild weather with significant cloud cover: ‘**Temperate and Cloudy**’. During this period, the temperature dynamics during warmer weather, could be assessed, where the effects of solar heat gain are minimised.
 - o 27th of May until 30th of May

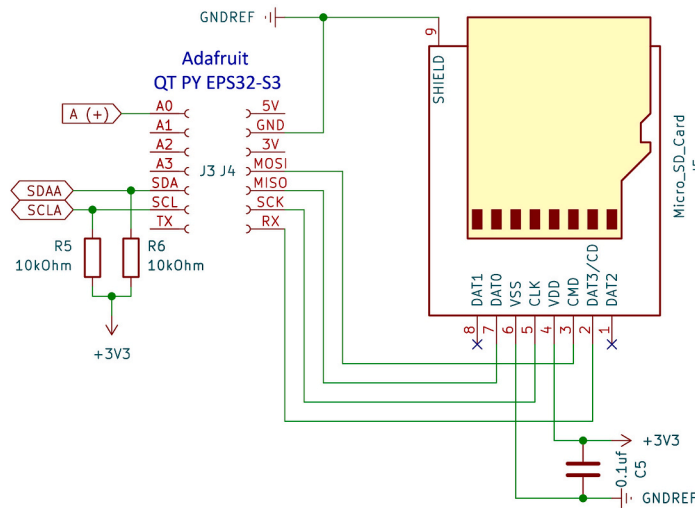
CONNECTOR BOARD



Connector board
USB C power delivery (+5V & +3V3)

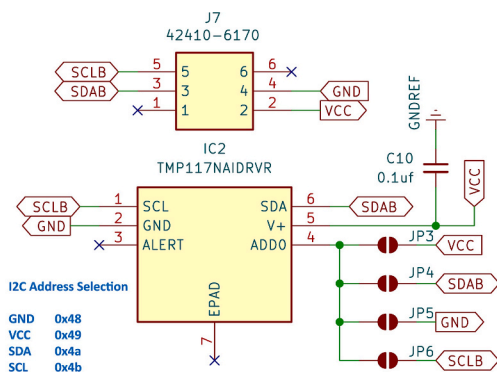


Connector board
Sensor buffer, level shifter and I2C address selection

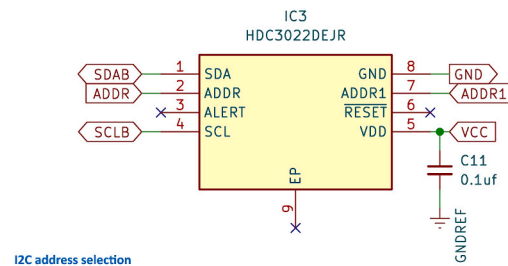


Connector board
Connection between microcontroller board plus SD card reader

SENSORS



Material temperature sensor
TMP117 based with RJ11 connector



Air temperature sensor
HDC3022 based with soldered cable connection

Fig. 3. Circuit diagrams of the custom sensors and datalogger used in this experiment.



Fig. 4. Experimental set-up in the Hortus Botanicus Delft showcasing the location of the different sensors and samples.

- o Average daytime temperature: 16.9 °C; average nighttime temperature: 13.6 °C
- A period of hot and dry weather with minimal cloud cover and rain: **'Hot and Sunny (Dry)'**. In this period, the temperature dynamics during warm weather and under strong sunlight could be assessed when the moss is not hydrated, thus no evaporative cooling can take place.
 - o 12th of June until 15th of June
 - o Average daytime temperature: 24.3 °C; average nighttime temperature: 18.2 °C
- A period of hot weather with minimal cloud cover, during which this time each sample was manually sprayed with 40 mL of tap water once a day, a value chosen based on the amount of water the moss could absorb in a short period of time without surface run-off: **'Hot and Sunny (with Watering)'**. This period had relatively similar weather to the previous period, but this time the effect of any potential evaporative cooling could be assessed.
 - o 16th of June until 19th of June
 - o Average daytime temperature: 22.7 °C; average nighttime temperature: 15.4 °C

For these periods, infrared images taken with the FLIR Lepton 3.5 camera were collected and batch-analysed in the FLIR Thermal Studio software, by placing a 20x20pixel measurement rectangle in the middle of each sample, from which the average surface temperature value was obtained using an $\epsilon = 0.95$ emissivity setting. These values were exported to Microsoft Excel, and for each set of three samples with the same treatment, the sample value was averaged for each picture to obtain an average surface temperature for each treatment for every 10-

min period. Similarly, for the temperature sensors, the data from the material temperature (TMP117) and air temperature (HDC3022) were collected and averaged for each treatment and sensor type. The measurements from the two ambient light sensors (VEML7700) and the two ambient air temperature sensors (HDC3022) were also averaged across both sensors. To obtain average day and night values, the average value for each treatment was calculated based on local sunrise and sunset times. Whereas the maximum and minimum temperatures are based on the highest and lowest daily value for each sample respectively, which was then averaged for each treatment.

To determine statistically significant differences between the different treatments several Kruskal-Wallis analyses were performed in R version 4.4.3 (R Core Team, 2023) using the 'PMCMRplus' package (PMCMRplus: Calculate Pairwise Multiple Comparisons of Mean Rank Sums Extended, 2024), with the different temperature parameters as the dependent variable and *Treatment* as the independent variable. For significant results ($p < 0.05$) a post-hoc Conover-Iman test with a Benjamini-Hochberg correction was also performed. The post hoc results were used to create homogeneous subsets with an alpha level of 0.05.

3. Results

A full overview of the average daytime and nighttime temperatures can be found in the Supplementary Materials, whereas a summary per measuring period can be found in Table 3. In the rest of this chapter, the measuring results from the air temperature sensors (TI HDC3022), infrared sensor (FLIR Lepton 3.5) and material temperature sensors (TI TMP117) will be discussed separately.

Table 3

Average daytime, nighttime, maximum, and minimum temperature for the different treatments during the different weather conditions, including test statistics from the Kruskal-Wallis statistical analysis. Significant p-values (<0.05) are highlighted in bold. For significant results, the homogeneous subsets based on the post-hoc Conover-Iman tests are denoted by the letter next to the temperature, with treatments sharing on or more letters denoting the difference between those treatments is not significant ($p > 0.05$). If a treatment differs significantly from the bare bioreceptive reference (**Bioref**) they are highlighted in blue in case the temperature is lower, or red if the temperature is higher. Reported air temperatures are those measured by the temperature sensors just above the surface of the mortar sample, surface temperatures are those reported by the infrared camera, and material temperatures are those measured by the primary temperature sensor inside the samples. Treatments are marked as follows: samples fully covered with the moss *G. pulvinata* (**GP**), *P. capillare* (**PC**), or *B. rutabulum* (**BR**), samples partially covered with the moss *G. pulvinata* (**GPP**), samples covered by the climbing plant *H. helix* (**HH**) and samples covered with both the moss *G. pulvinata* AND the climbing plant *H. helix* (**HH + GP**).

Weather conditions	Treatment	Air temperature				Surface (IR) temperature				Material temperature			
		Day		Night		Day		Night		Day		Night	
		avg.	avg.	Max	Min	avg.	avg.	Max	Min	avg.	avg.	Max	Min
Cold Weather	Bioref	2.7	0.1	6.2	-3.1	5.0 ^a	2.5	8.1 ^a	-1.9	2.2 ^a	1.6	5.5 ^a	-1.6
	GP	2.6	0.0	5.9	-3.1	6.3 ^c	2.2	8.8 ^b	-2.3	0.7 ^b	0.9	3.7 ^b	-1.8
	PC	2.6	-0.1	6.1	-3.2	6.1 ^{bc}	2.1	8.6 ^{ab}	-2.3	0.7 ^b	0.9	3.6 ^b	-1.6
	BR	2.7	0.0	6.0	-3.2	6.2 ^c	2.4	8.8 ^b	-2.0	0.9 ^b	1.1	4.0 ^b	-1.7
	GPP	2.6	0.0	6.0	-3.2	5.5 ^{ab}	2.5	8.2 ^{ab}	-1.9	1.5 ^a	1.1	4.8 ^a	-2.1
	HH	2.7	0.0	6.1	-3.2	5.5 ^{ab}	2.7	8.4 ^{ab}	-1.7	1.5 ^a	0.9	4.9 ^a	-2.3
	HH+GP	2.6	0.0	6.0	-3.2	5.8 ^{bc}	2.5	8.5 ^{ab}	-2.0	0.7 ^b	1.1	3.7 ^b	-1.5
	Kruskal- Wallis	X ² p	6.55 0.478	1.79 0.971	2.88 0.901	0.87 0.997	19.14 0.008	11.59 0.12	14.79 0.039	13.53 0.060	16.52 0.021	1.93 0.963	17.34 0.015
Temperate and Cloudy Weather	Bioref	17.4	13.5	24.2	11.4	18.9	15.3	23.8 ^a	13.3	19.4	16.4	23.4	14.9
	GP	17.2	13.6	23.8	11.6	19.5	15.1	28.3 ^{bcd}	12.9	18.2	16.7	21.0	15.2
	PC	17.3	13.6	24.3	11.6	19.7	15.1	29.4 ^b	12.9	18.2	16.8	21.0	15.2
	BR	17.6	13.7	24.6	11.8	19.6	15.2	28.4 ^{bc}	12.9	18.8	17.4	21.7	15.8
	GPP	17.3	13.6	23.8	11.5	19.4	15.4	26.1 ^d	13.3	18.3	15.8	21.9	14.4
	HH	17.4	13.5	24.3	11.6	18.6	15.3	23.3 ^a	13.2	18.5	16.0	22.0	14.7
	HH+GP	17.3	13.6	23.6	11.6	19.1	15.0	27.0 ^{cd}	12.8	17.3	16.0	19.8	14.5
	Kruskal- Wallis	X ² p	7.00 0.429	3.44 0.842	9.80 0.200	5.12 0.645	13.61 0.059	4.64 0.704	19.71 0.006	10.11 0.183	3.48 0.837	6.57 0.476	8.76 0.271
Hot and Sunny Weather (Dry)	Bioref	26.7 ^a	14.9	37.9 ^a	14.8 ^a	29.6 ^a	17.9 ^{ab}	40.2 ^a	17.2	29.6	19.1 ^a	38.7 ^a	18.2 ^{ab}
	GP	27.3 ^{ab}	15.7	39.4 ^{abc}	15.3 ^b	33.7 ^b	17.9 ^{ab}	59.4 ^b	17.5	30.5	22.9 ^b	37.1 ^{ab}	20.6 ^a
	PC	27.3 ^{ab}	15.5	40.2 ^{bc}	15.2 ^{ab}	33.6 ^b	17.6 ^a	58.6 ^b	17.2	30.0	22.1 ^b	36.4 ^{abc}	20.1 ^a
	BR	27.7 ^b	15.4	40.6 ^b	15.2 ^{ab}	31.1 ^c	17.5 ^a	48.5 ^c	17.1	29.9	22.2 ^b	36.1 ^{bc}	20.4 ^a
	GPP	26.9 ^a	15.2	38.7 ^{bc}	15.0 ^{ab}	31.7 ^c	18.2 ^b	47.4 ^c	17.5	29.8	19.8 ^{bc}	38.6 ^a	18.4 ^{ab}
	HH	26.8 ^a	15.0	38.5 ^a	14.8 ^a	28.6 ^a	17.6 ^a	38.4 ^a	17.0	27.6	18.4 ^a	35.3 ^{bc}	17.3 ^b
	HH+GP	27.4 ^{ab}	15.4	40.5 ^{bc}	15.2 ^{ab}	30.9 ^c	17.5 ^a	47.8 ^c	17.0	28.2	21.2 ^{bc}	33.9 ^c	19.3 ^{ab}
	Kruskal- Wallis	X ² p	16.09 0.024	12.23 0.093	17.45 0.015	16.49 0.021	21.25 0.003	14.48 0.043	21.35 0.003	11.59 0.115	13.75 0.056	19.35 0.007	17.33 0.015
Hot and Sunny Weather (with watering)	Bioref	25.2 ^a	18.2 ^a	36.6	13.1	27.5 ^{ab}	21.2	37.5 ^a	15.3 ^{ab}	27.5	22.3 ^{ab}	36.6 ^a	16.2 ^{ab}
	GP	25.8 ^{ab}	18.6 ^b	38.1	13.8	31.2 ^c	21.0	56.6 ^b	15.7 ^a	28.6	25.1 ^c	34.7 ^{abc}	19.0 ^b
	PC	25.8 ^{ab}	18.4 ^{ab}	38.7	13.7	30.8 ^{cd}	20.8	55.4 ^b	15.4 ^{ab}	27.8	24.6 ^c	33.8 ^{bcd}	18.3 ^b
	BR	26.2 ^b	18.5 ^{ab}	38.9	13.6	28.5 ^{cd}	20.6	46.8 ^c	15.4 ^{ab}	28.2	24.8 ^{bc}	34.5 ^{bc}	18.4 ^b
	GPP	25.3 ^a	18.3 ^{ab}	37.2	13.4	29.0 ^{ab}	21.3	43.5 ^d	15.7 ^a	27.5	22.6 ^{ab}	35.9 ^{bc}	16.5 ^{ab}
	HH	25.3 ^a	18.2 ^a	37.0	13.2	26.4 ^a	20.9	35.7 ^a	15.2 ^{ab}	25.7	21.3 ^a	33.6 ^{cd}	15.5 ^a
	HH+GP	25.9 ^{ab}	18.4 ^{ab}	38.9	13.6	28.3 ^{cd}	20.5	45.4 ^{cd}	15.4 ^{ab}	26.2	23.5 ^{bc}	31.7 ^d	17.6 ^{ab}
	Kruskal- Wallis	X ² p	15.40 0.031	14.59 0.042	13.37 0.064	12.49 0.085	20.56 0.004	12.92 0.074	21.8 0.002	14.48 0.043	12.88 0.075	17.11 0.017	17.84 0.013

3.1. Local air temperature

Based on the experimental hypotheses, moss was expected to affect air temperatures in the near-surface air layer only when the moss is exposed to direct sunlight (increasing temperatures) or when evapotranspiration occurs (decreasing temperatures). Indeed, as shown in Table 3, during the *Cold*, and *Temperate and Cloudy* periods, sunlight intensity was relatively low, and the effect of moss coverage on air temperatures was mostly minimal and not statistically significant. During the *Cold* period, the observed near-surface air temperatures of all moss-covered samples were slightly lower than those of the bare bioreceptive samples and the samples covered by only *H. helix* (Table 3). However, differences were very small (0.0 °C to −0.1 °C), and the air temperature in front of all samples mostly followed the ambient air temperature (Fig. 5a).

During the *Temperate and Cloudy* period, average differences between the moss-covered samples and the bare bioreceptive samples, as well as those covered with *H. helix*, were again small (−0.2 °C to +0.2 °C) and not statistically significant. However, this time, the air in front of the moss-covered samples was no longer always cooler, especially for those covered with *B. rutabulum* (Table 3). Instead, the near-surface air temperature no longer strictly tracked the ambient air temperature, as temperature spikes can be observed during periods of sunlight (Fig. 5b), leading to slightly higher average maximum temperatures for some samples, although these differences were again not statistically significant (Table 3).

The effect of sunlight on near-surface air temperature became more pronounced during the *Hot and Sunny (Dry)* period. Temperature differences of +10 °C or more were observed between the ambient air temperature and the air temperature in the near-surface air layer of all samples during the direct sunlight exposure (Fig. 5c). However, this effect was particularly pronounced for the moss-covered samples, as average maximum temperatures of the moss-covered samples were significantly higher (+1.5 °C to +2.7 °C) than the bare bioreceptive reference (Table 3). The differences in average daytime near-surface air temperatures were lower at +0.5 °C (*GP*), +0.7 °C (*PC*), or +1.0 °C (*BR*) above those of the bare bioreceptive samples, with only *B. rutabulum* showing a difference that was statistically significant (Table 3). When the panel was only partially covered with *G. pulvinata*, the difference was reduced to +0.2 °C; however, the difference increased to +0.7 °C when *G. pulvinata* was combined with *H. helix*. During the night, the average difference between the bare and moss-covered samples was reduced to +0.5 °C to +0.8 °C and no longer statistically significant (Table 3), although overall near-surface air temperatures remained somewhat higher in front of the moss-covered samples throughout the night (Fig. 5c). For the samples with only *H. helix*, both the average day (+0.1 °C) and nighttime (0.0 °C) near-surface air temperatures, as well as the maximum and minimum temperatures were almost identical to those of the bare bioreceptive samples.

Providing manual watering during the *Hot and Sunny (with Watering)* period only made a temporary difference to the air temperatures. While watering led to an initial sharp decrease in near-surface air temperatures of the moss-covered samples, leading to air temperatures that can be below those of the bare bioreceptive samples (Fig. 5d), this effect was very short-lived. Subsequently, near-surface air temperatures of the moss-covered samples quickly rose again to values above those of the bare bioreceptive samples (Fig. 5d). Overall, average differences in daytime near-surface air temperature between the moss-covered samples and the bare bioreceptive samples were nearly identical to those during the period where no water was provided (+0.6 °C to +1.0 °C). In contrast, during the nighttime, differences in average air temperature were significant, with the air in front of the moss-covered samples somewhat cooler relative to the bare bioreceptive samples than it was before (+0.2 °C to +0.4 °C). However, this may be due to the lower nighttime ambient air temperature during this period. As for the sample using only *H. helix*, the difference between it and the bare bioreceptive

sample was once again very minimal.

3.2. Surface temperatures

Based on the initial hypotheses, sunlight exposure and evapotranspiration were expected to, respectively, increase and decrease surface temperatures of the moss-covered samples compared to bare concrete. As shown in Fig. 6a, although only two days of the *Cold* period were recorded due to early software teething issues, the pattern during those two days was already clear. During the day, the surface temperature of the bare bioreceptive samples stayed slightly below the ambient air temperature, whereas the surface temperature of the moss-covered samples responded more quickly to both an increase in ambient air temperature and sunlight. This resulted in a statistically significant average daytime surface temperature difference of +1.1 °C to +1.3 °C compared to the bare bioreceptive samples, with the highest temperatures observed on the *GP* samples and the lowest on the *PC* samples (Table 3). When the sample was only partially covered with moss or covered with both moss and *H. helix*, the difference dropped to +0.5 °C or +0.8 °C, respectively. Samples only covered by *H. helix* were on average +0.5 °C warmer than the bare bioreceptive samples during the daytime, although this difference was not statistically significant.

During the night, the reverse effect was observed. The surface temperature of the moss-covered samples decreased more rapidly than that of both the bare bioreceptive samples, resulting in an average nighttime surface temperature difference of −0.4 °C to −0.1 °C, although this difference was not statistically significant. The highest average temperatures were observed on the *BR* samples, and the lowest on the *PC* samples. This time, partial moss coverage or the combination of moss with *H. helix* resulted in similar surface temperatures to those of the bare bioreceptive samples, and coverage with only *H. helix* led to a small increase in surface temperature (+0.2 °C).

The same overall pattern could be observed for all other weather types as well. Higher daytime surface temperatures, following the rising ambient air temperatures and increased sunlight, with significantly higher peak temperatures (Table 3) and lower nighttime surface temperatures as the sun sets, and the ambient air temperatures are lower (Fig. 6b-d). However, although the patterns are similar, the differences in surface temperature become more pronounced with increasing sunlight intensity. This resulted in daytime surface temperature differences of +0.6 °C to +0.8 °C for the completely moss-covered samples compared to the bare bioreceptive samples during the *Temperate and Cloudy* period that fell just short of statistical significance (Table 3), although peak temperatures were significantly higher at +4.5 °C to +5.6 °C and nighttime surface temperature differences of −0.2 °C to −0.1 °C that were similarly not statistically significant. This increased to a statistically significant +1.5 °C to +4.1 °C during the *Hot and Sunny (Dry)* period in the daytime, and to −1.0 °C to −0.3 °C at night. These higher average daytime differences were primarily due to high surface temperatures under direct sunlight, resulting in maximum temperature differences of on average +19.2 °C (*GP*), +18.4 °C (*PC*), and +8.3 °C (*BR*). The average differences between the moss-covered samples and the bare bioreceptive samples were slightly reduced when manual watering was provided, ranging from +1.0 °C to +3.7 °C during the day and from −0.4 °C to 0.0 °C at night, at which point the differences were no longer statistically significant (Table 3). Overall, the samples covered by the acrocarpous moss species *G. pulvinata* and *P. capillare* recorded significantly higher daytime and maximum surface temperatures during these warmer periods than those covered by the pleurocarpous species *B. rutabulum*, mostly in response to sunlight.

Samples with partial moss coverage were slightly cooler during the day than their fully covered counterparts, although they remained significantly warmer than the bare bioreceptive samples (Table 3). The samples that combined moss with *H. helix* had even lower surface temperatures, yet daytime surface temperatures were still above those of the bare bioreceptive samples, although when combined with watering, the

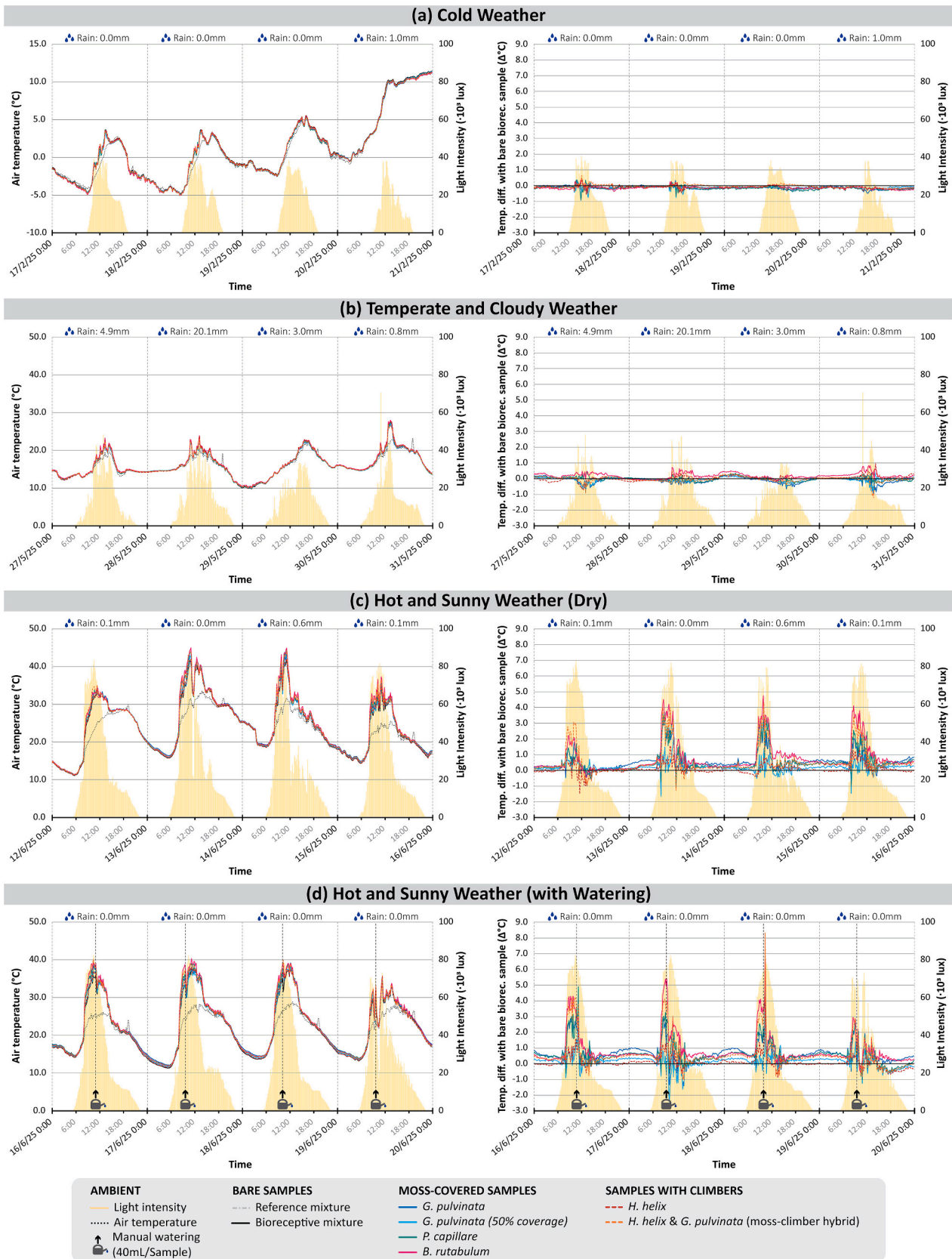


Fig. 5. Averaged absolute and relative (to the bare bioreceptive samples) near-surface air temperatures of the moss-covered samples during (a) cold weather, (b) temperate and cloudy weather, (c) hot and sunny weather, and (d) hot and sunny weather during which the samples were manually watered. Also included are ambient air temperature and light intensity values, as well as absolute air temperature values for the bare reference and bioreceptive samples.

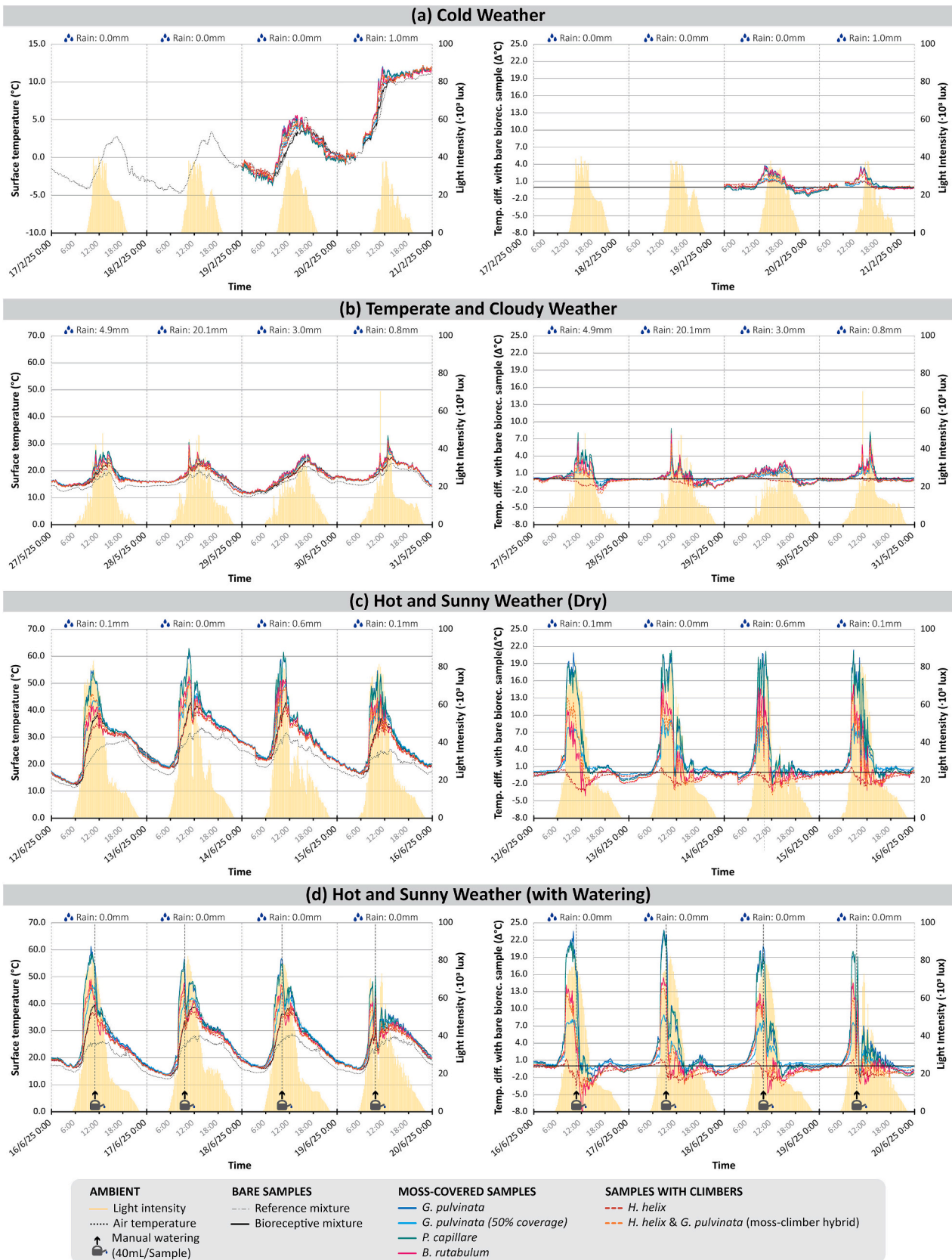


Fig. 6. Averaged absolute and relative (to the bare bioreceptive samples) surface temperatures (IR) of the sample during (a) cold weather, (b) temperate and cloudy weather, (c) hot and sunny weather, and (d) hot and sunny weather during which the samples were manually watered. Also included are ambient air temperature and light intensity values, as well as absolute surface temperature values for the bare reference and bioreceptive samples.

daytime difference was no longer statistically significant (Table 3). The only samples that had daytime surface temperatures that were consistently below those of the bare bioreceptive samples were the *H. helix*-only samples, with surface temperatures that were on average -0.3 °C, -1.0 °C, and -1.0 °C below those of the bare bioreceptive samples during the *Temperate and Cloudy*, *Hot and Sunny (Dry)*, and *Hot and Sunny (with Watering)* periods, respectively, yet these differences were too small to be statistically significant (Table 3). During nighttime, both *H. helix* treatments (*HH*, and *HH + GP*) showed surface temperatures below those of the bare bioreceptive samples. However, the combination of moss with *H. helix* showed the lowest overall temperatures.

3.3. Material temperature inside the mortar substrate layer

Stemming from the initial hypotheses, moss was expected to have a mediating effect on substrate temperatures. And indeed, as can be seen in Fig. 7, while the moss covering caused both higher peak surface and air temperatures during periods of higher sunlight intensities, the reverse held true for the temperature inside the mortar base layer of the samples. Peak material temperatures of the moss-covered samples were (sometimes significantly) lower than those of the bare bioreceptive samples. Furthermore, it also took a longer time to reach these peak temperatures, as can be inferred from the flatter absolute temperature slopes of the moss-covered samples and the negative temperature differences with the bare bioreceptive samples during the mornings, as shown in Fig. 7. The opposite also held true, however, as the moss-covered samples were also slower to lose their internal heat during periods when the ambient temperature was lower, and the sun was not shining, leading to positive temperature differences with the bare bioreceptive samples during the late afternoon and/or night.

The experimental results showed that this led to average daytime temperatures inside the mortar base layer of the moss-covered samples being -1.5 °C to -1.3 °C lower than those of the bare bioreceptive samples during the Cold period (Table 3). The differences were smaller and no longer significant at -1.2 °C to -0.6 °C lower during the *Temperate and Cloudy* period, coinciding with a much smaller difference between daytime and nighttime ambient temperatures (Fig. 7b). During the *Hot and Sunny (Dry)* period, the average maximum internal temperatures of the moss-covered samples were still -1.6 °C (*GP*), -2.3 °C (*PC*), or even -2.6 °C (*BR*) below those of the bare bioreceptive samples during periods of direct sunlight, but average daytime temperatures of the internal material were now $+0.3$ °C to $+0.9$ °C above those of the bare bioreceptive samples, mainly due to higher temperatures in the late afternoon (Fig. 7c). Providing manual watering somewhat increased these differences to $+0.3$ °C to $+1.1$ °C, with temperatures increasing relative to the bare bioreceptive samples directly after the watering events, whereas maximum temperatures were lower relative to the bare bioreceptive reference samples than before for the acrocarpous species at -1.9 °C (*GP*), -2.8 °C (*PC*), and slightly higher for the pleurocarpous species at -2.1 °C (*BR*). This can also be observed in Fig. 7d, where the relative temperature drop after watering appears somewhat stronger for the acrocarpous species. Throughout all testing periods, the *PC* samples showed the lowest overall daytime material temperatures, with *GP* recording the highest temperatures during both *Hot and Sunny* periods, and *BR* during the *Cold* and *Temperate and Cloudy* periods.

During the nighttime, the internal temperatures of the moss-covered samples were consistently and significantly higher than those of the bare bioreceptive samples, except during the Cold period, when they were on average -0.5 °C to -0.7 °C lower (Table 3). During the *Temperate and Cloudy* period, the differences with the bare bioreceptive samples were relatively small at $+0.3$ °C to $+1.1$ °C; however, this increased to $+2.3$ °C to $+2.8$ °C during the *Hot and Sunny* period, and even further to $+3.0$ °C to $+3.9$ °C during the *Hot and Sunny (Dry)* period with additional manual watering. During the nighttime, the *PC* samples were once again the coolest during both *Hot and Sunny* periods, although this time *GP* was slightly cooler during the *Temperate and Cloudy* period and *BR*

during the *Cold* period (Table 3). The treatments with the highest internal temperatures were *GP* during both *Hot and Sunny* periods, *BR* during the *Temperate and Cloudy* period, and both *GP* and *PC* during the *Cold* period.

The samples with only partial moss coverage exhibited mortar temperatures that fell somewhere between those of the completely moss-covered samples and those of the bare bioreceptive samples (Table 3). Samples covered with *H. helix*, on the other hand, recorded temperatures that were consistently below those of the bare bioreceptive samples, regardless of the testing period, although the differences were too small to be statistically significant (Table 3). The moss and *H. helix* hybrid showed more volatile results. These samples consistently recorded the lowest peak daytime temperatures, although similar to the regular moss-covered samples, temperature changes happen more slowly. This resulted in average daytime and nighttime temperatures below those of the samples with only *H. helix* during the *Temperate and Cloudy* period, but higher average daytime and nighttime temperatures during the *Hot and Sunny* periods. However, in both cases, these values were still lower than those of the samples covered only by moss.

One final observation is that, unlike the air and surface temperature measurements, where there was little to no difference between the normal and bioreceptive reference mixes, the internal material temperatures of the normal reference mix are notably lower, by up to 1.4 °C, compared to those of the bioreceptive mix (Fig. 7).

4. Discussion

The main effect on temperatures of most conventional vertical greenery systems is the interception of solar radiation, thereby reducing the surface heating of the underlying material (Pérez et al., 2011; Kontoleon and Eumorfopoulou, 2010; Ip et al., 2010). This shading effect on the temperature of the mortar surface could not be directly observed in this experiment, as the thermal camera used could only measure the temperature of the outermost layer – in this case, the leaves of the *H. helix* – and not that of the shaded underlying mortar. Consequently, peak daytime surface temperatures were similar for both the bare bioreceptive samples and those covered by the climbing plant. However, the latter exhibited a somewhat faster reduction in surface temperature during the late afternoon and evening, most likely due to the lower thermal mass of the *H. helix* leaves compared to the mortar. One of the consequences of the lower surface temperature of the shaded mortar can be observed in the internal material temperatures of the samples, as both the peak temperatures inside the *H. helix*-covered samples were significantly lower than those of the bare reference samples during sunny days, even though the differences in average temperature were not large enough to be statistically significant. Since both sample types were composed of the same material, with comparable thermal conductivity and storage properties, this difference in conductive heat flux [Q_G] and resulting heat storage [ΔQ_S] must be driven by a variation in surface temperature (Fig. 1), caused by shading of the surface by *H. helix*. Apart from this effect, the thermal dynamics of the bare and *H. helix* samples were largely similar, with no observable insulating effect by the *H. helix*. The effect of the application of moss, on the other hand, was altogether different from that of *H. helix*.

4.1. Increased temperatures under sunlight

The first expected effect of moss application was that its low albedo would increase temperatures under sunny conditions. And indeed, once sunlight hit the moss-covered samples, the surface temperature rapidly increased, reaching peak temperatures that could be 20 °C or more above those of the bare bioreceptive samples in individual cases. These extreme surface temperatures, however, are in line with values reported in natural moss communities, where moss surface temperatures that are 5 °C to 25 °C above the ambient air temperature have regularly been recorded, and even differences of more than 40 °C have been observed

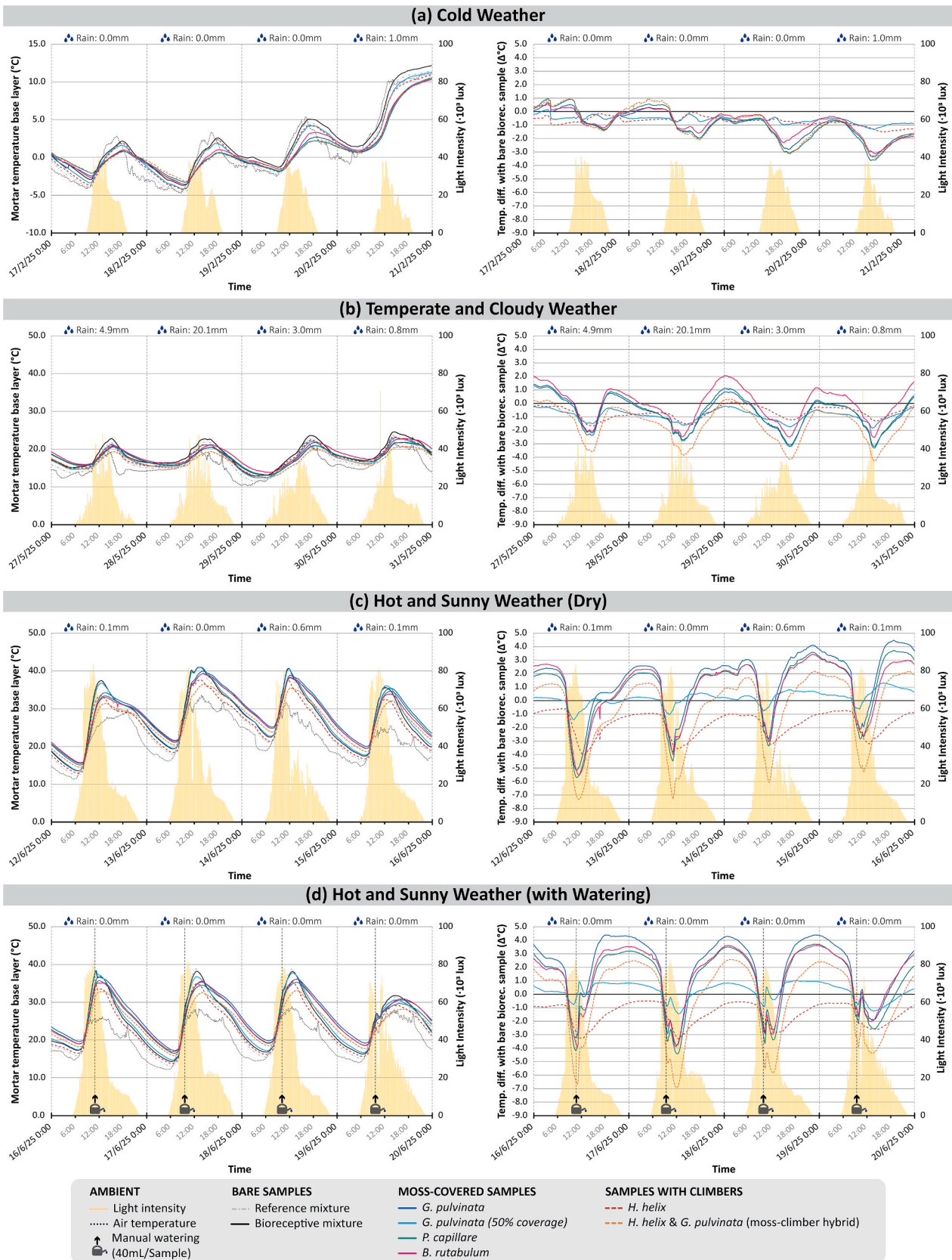


Fig. 7. Averaged absolute and relative (to the bare bioreceptive samples) substrate temperatures in the middle of the mortar samples during (a) cold weather, (b) temperate and cloudy weather, (c) hot and sunny weather, and (d) hot and sunny weather during which the samples were manually watered. Also included are ambient air temperature and light intensity values, as well as absolute surface temperature values for the bare reference and bioreceptive samples.

(Block et al., 2009). This increased both the sensible heat flux [Q_H] and the outgoing long-wave radiation [$L\uparrow$] (Fig. 1), causing an increase in the near-surface air temperature and mean radiant temperature, respectively, which in turn could cause an increase in heat stress in humans (Havenith and Fiala, 2015). However, in practice, the increase in air temperatures was limited to 1.0 °C on average at most, and only statistically significant for *B. rutabulum* during the warmer testing periods. Furthermore, the extent of this heating effect was also observed to be species dependent in this study, with heating under sunlight being stronger for the acrocarp species (*G. pulvinata* and *P. capillare*) than for the pleurocarp species (*B. rutabulum*). This might have been caused by differences in albedo, as previous research has found an albedo range of 0.07 to 0.22 for moss (Xiao and Bowker, 2020; Amir et al., 2018; Stache et al., 2022; Williamson et al., 2016; Petzold and Rencz, 1975), depending on species and hydration level (Xiao et al., 2019; Petzold and Rencz, 1975; Stoy et al., 2012). It should also be noted that this heating effect is strongly linked to sunlight intensity. Once the direct sunlight disappeared in the late afternoon, moss surface temperatures quickly dropped to similar levels as the bare samples, and even dropped slightly below the bare sample values during the night, leading to large temperature fluctuations between day and nighttime, similar to those recorded in natural moss communities (Stoy et al., 2012). This can be explained by the low volumetric heat capacity, thermal conductivity, and high thermal diffusivity of moss compared to concrete (Xiao et al., 2019; Shafiqh et al., 2020), leading to a comparatively smaller amount of heat energy being stored in the moss, which can then be lost more easily. Additionally, during periods of lower sunlight intensity (the cloudy and temperate spring period, or cold winter period) or when the moss was shaded by another object (as is the case for the samples with

the combined moss and climber coverage), the surface temperature difference between the moss-covered and the bare samples is much reduced. Finally, the effect of these increased surface temperatures on air temperature appeared limited. Moreover, as in this research, only air temperature directly in contact with the moss or material surface was measured, and its effect was found to be negligible, only a marginal influence on air temperature at a larger distance from the moss surface can be expected.

4.2. The insulating effects of moss

The second effect hypothesised was that temperature fluctuations within the underlying substrate (the mortar) would be reduced due to the insulating properties of moss being higher than those of mortar, and this was confirmed by the experimental findings. As the moss was directly connected to the mortar samples, one would expect the high surface temperature of the moss to also lead to an increase in the internal temperature of the sample, as the conductive heat flux [Q_G] is linked to the temperature difference between the material surface and its interior temperature (Fig. 1). Although the average daytime temperature of the base material was indeed higher than that of the moss-covered samples (caused by the high surface temperature of moss when exposed to sunlight), the peak daytime temperatures were slightly lower. Furthermore, whereas the internal temperature of the bare samples closely followed their surface temperature, this was not the case for the moss samples. Once the surface temperature increased, the interior temperature of the underlying mortar rose only slowly, and vice versa, reducing the amplitude of the temperature fluctuations within the base layer (Fig. 8). This insulating effect is similar to that observed in natural ecosystems,

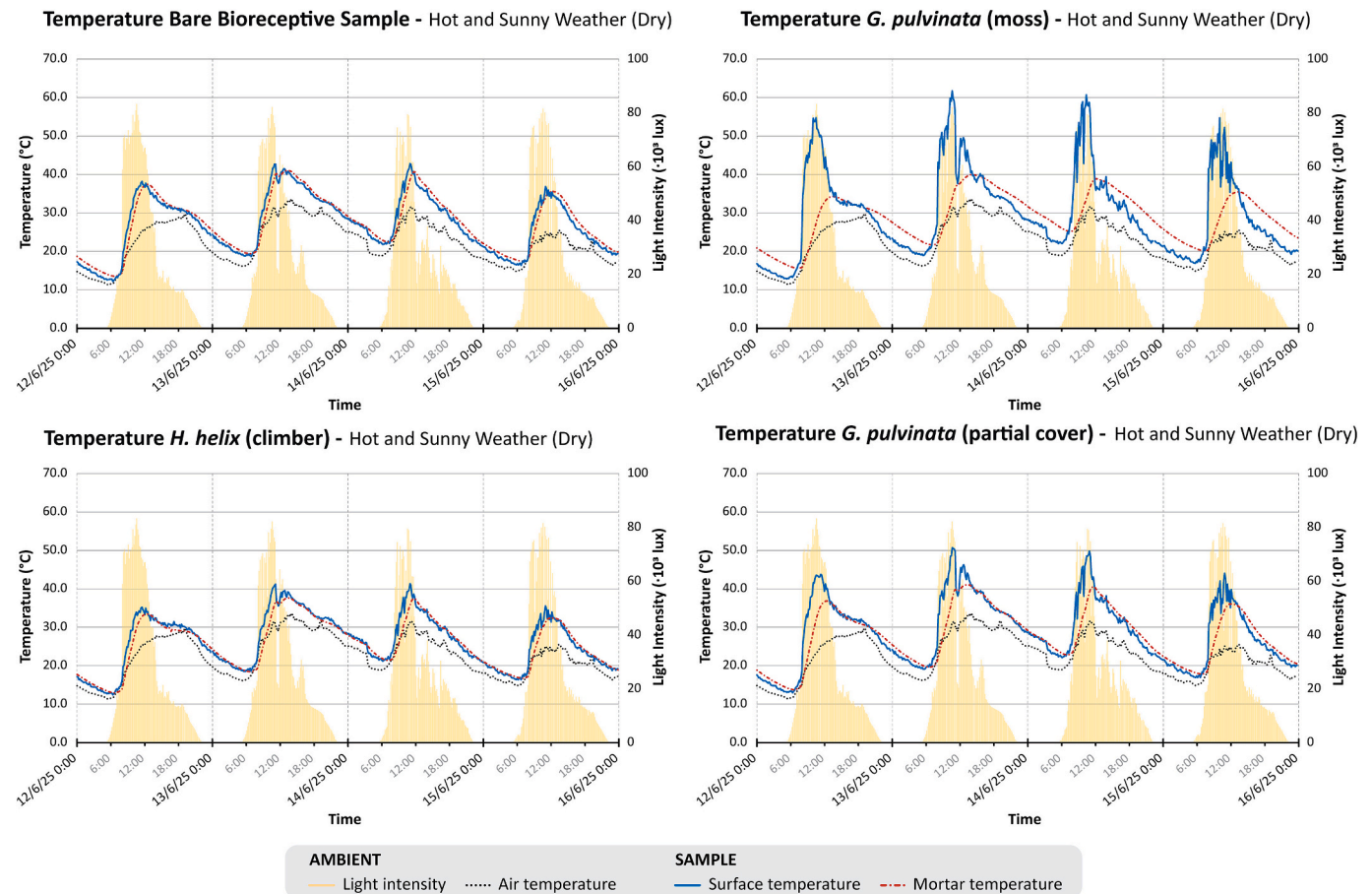


Fig. 8. Graphs comparing the interaction between the temperature of the surface of the sample and that of the mortar temperature of the base layer for the bare bioreceptive, full moss-covered, partially moss-covered, and climber-covered panels.

where the presence of moss coverage dampens the temperature fluctuations in the underlying soil, although the extent to which is dependent on mat density, thickness and moisture level (Xiao et al., 2019; Soudzilovskaia et al., 2013; Blok et al., 2011; Koranda and Michelsen, 2021; Gornall et al., 2007). This insulating effect is not enough, however, to fully mitigate the surface heating under sunlight to reach the underlying mortar. As mentioned before, under sunny conditions, the mortar still reached average daytime temperatures higher than those seen in the bare samples. Subsequently, the insulating properties of the moss also meant that this heat energy could not easily be lost at night, leading to mortar temperatures that were even higher relative to the bare bio-receptive samples. Furthermore, the samples with only partial moss coverage highlight the importance of continuous moss coverage for this effect, as these gaps significantly compromise the insulation provided by the moss. This led to the leakage of heat energy around the moss (Fig. 9), similar to gaps in conventional insulation (O'Hegarty et al., 2024). This subsequently resulted in temperature fluctuations within the underlying mortar layer that were more similar to those of the bare samples (Fig. 8).

4.3. The cooling effect of evapotranspiration

Finally, a surface-cooling effect of moss due to evapotranspiration of hydrated moss was hypothesised. Although the experimental results showed that watering off the moss surface drastically reduced its surface temperature and somewhat reduced the near-surface air temperature, both in absolute terms and relative to the bare bio-receptive samples, this effect was very short-lived. As evaporation rates in moss are linked to moss temperature relative to ambient air temperatures (Bond-Lamberty et al., 2011), the high moss temperatures at the time of application may have caused the majority of the water to evaporate quickly, after which temperatures began to rise again. Furthermore, whereas watering led to

a reduction in surface and local air temperatures, the temperature gain inside the mortar samples increased relative to the bare samples, suggesting that the increase in moisture reduced the insulating effects of moss, which is in line with previous findings (Xiao et al., 2019; Soudzilovskaia et al., 2013; O'Donnell et al., 2009b).

4.4. Practical implications

Our findings showed two main effects on temperatures. Due to its low albedo, a moss surface tends to rapidly increase in temperature under direct sunlight. At the same time, its insulating properties also reduce heat fluxes to and from the interior walls, thereby stabilising the temperature of the underlying substrate. Although the tests were performed on a small-scale controlled setup, these effects are likely to persist qualitatively, as they are caused by the inherent properties of the moss, particularly albedo and thermal conductivity, which are mostly scale-agnostic. However, the magnitude of the temperature differences caused by the moss can be expected to vary depending on the scale of the system, but also on the local weather conditions. This is particularly true for the effect the moss has on air temperatures. In this experiment, the effect of moss on air temperatures was found to be minimal; however, there are two caveats. First, the temperature was recorded close to the surface, at a distance of 5 mm, due to the small scale of this experiment. This means only the air temperature in the surface boundary layer was recorded. As such, at larger distances, which are more relevant for urban scales, the temperature effects would be strongly reduced as the convective heat is dispersed over a larger air volume. At the same time, due to the limited surface area of the moss, only a marginal absolute heat flux was provided to the air. When used on larger surfaces, this could lead to a more significant amount of energy being transferred from the wall. Therefore, further large-scale testing is necessary to determine the

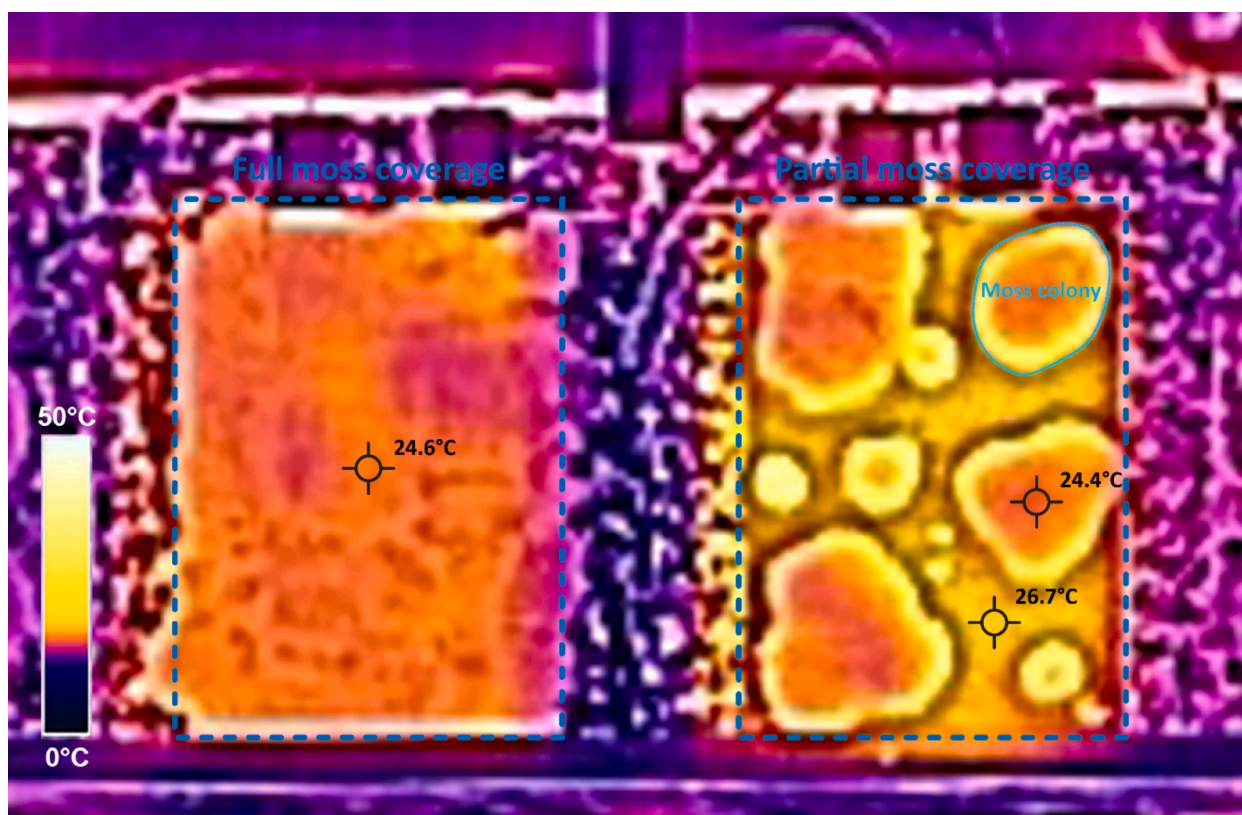


Fig. 9. Infrared image showing the difference in surface temperature between a sample with full-moss coverage (left) and one with partial moss coverage (right), in the evening (22:30), following a hot and sunny day on the 12th of June 2025. The surface of the moss colonies on the sample with partial moss coverage is similar to that of the panel with full coverage; however, the surface temperature of the exposed mortar in between the colonies is several degrees higher, suggesting significant heat loss between the moss colonies.

extent to which moss affects urban air temperatures, specifically. Furthermore, the testing periods in this experiment were kept relatively short (4 days each of stable weather) and chosen specifically to best test the hypothesised effects of moss on thermal dynamics. As such, the temperature effects of moss under varying weather patterns could not be determined. However, relatively minor daytime temperature fluctuations during the 'Cold' testing period already showed varying effects on substrate temperatures across the different treatments, warranting further research into how this pattern evolves across seasons and throughout the year.

Overall, the observed thermal effects of moss application differ from those of other vertical greenery systems. Climbing plants, as used in direct or indirect green façades, mainly provide cooling through shading, with a smaller evaporative cooling effect (Bakhshoodeh et al., 2022). Another vertical green typology, Living Wall Systems (consisting of a structure containing planter boxes or modular panels with plants), on the other hand, can affect temperatures through a combination of insulation, evaporative cooling and the reduction of solar heat gain (Azkorra-Larrinaga et al., 2023).

Based on these findings, moss-based greening systems could be particularly interesting in colder climates, where the heating effect under sunlight observed here can have a net positive effect on human health (Huang et al., 2023). At the same time, the strongest heating effect was observed in periods with high sunlight intensity, during which temperatures are already higher, and thus the surface heating effect is less positive, or even a net negative (Huang et al., 2023). However, the other properties of moss might still make it an interesting candidate for use in vertical greening solutions, also outside of colder climates. There are thermal insulation properties as found in this research, which may stabilise indoor temperatures, potentially reducing the energy required for heating and cooling. At the same time, it has also been found that moss exhibits good acoustic absorption and particulate matter capture, which are high compared to other plants (Veeger et al., 2025a; Haynes et al., 2019). And even in hotter climates, the surface heating effects may still be beneficial in colder seasons, as the net effect of urban heating can vary by season (Huang et al., 2023). Nonetheless, depending on the situation, the surface heating under sunlight exposure may need to be reduced.

In this case, one potential solution may be to keep the moss constantly hydrated. The findings in this research, specifically the increased daytime surface temperatures, differ from those of Perini, et al. (Perini et al., 2022), who found a daytime reduction in surface temperature for their moss-covered wall panels. This apparent discrepancy can most likely be explained by the fact that their system included an irrigation system that provided regular watering and used a textile intermediary substrate, which may have aided in increasing water absorption and retention. Similarly, Jongsoo and Jeasun (Jongsoo and Jeasun, 2026) found that using a moss covering reduced surface temperatures, but their system once again used an automated watering system with an unspecified substrate. In contrast, in our experiments, water was provided only once daily, and while the results showed a cooling effect from watering, this was very short-lived. As such, more frequent watering may be necessary to maintain temperatures consistently below the bare bioreceptive samples. Under the tested conditions, adding the equivalent of 0.67 L m^{-2} of water reduced temperatures under sun-exposed conditions for 1–1.5 h. Assuming a day of constant sunshine, this would mean several such watering events would be necessary. This compares to a water consumption of $3.37\text{--}12.69 \text{ L m}^{-2} \text{ d}^{-1}$ in Summer for a Living Wall System (Pérez-Urrestarazu, 2021), which additionally require year-round irrigation, whereas a moss-based system would only need to be irrigated when temperatures require it. However, as discussed before, keeping the moss hydrated will also reduce its insulating properties. This means that watering more frequently throughout the day may bring moss surface temperatures below those of a bare wall due to its high evaporation rate, but this will

come at the expense of its insulating properties. This means the watering regime will need to be fine-tuned depending on whether surface cooling or insulation is prioritised.

Instead, shading the moss either artificially or naturally may be better, as this avoids sun-induced surface heating while still maintaining the insulating properties of the moss. The potential of such a system could be observed in the samples that had a combined treatment of moss and *H. helix*, where the moss stabilised the interior temperatures of the samples, whereas the shading provided by the *H. helix* significantly reduced the surface temperatures of the samples, even though total leaf coverage was less than ideal, leading to surface temperatures that were still higher than the bare samples on the parts of the moss surface that were unshaded.

One final solution may lie in careful species selection, as the pleurocarp species *B. rutabulum* showed less strong surface heating in response to sunlight compared to the acrocarp species *G. pulvinata* and *P. capillare*, although it should be noted that *B. rutabulum*, in contrast to the two acrocarp species, is poorly adapted to high sunlight exposure conditions (Veeger et al., 2026).

5. Conclusion

This study aimed to investigate the effect of moss application on the thermal dynamics of a bioreceptive cementitious base material and compare these effects with those of a typical conventional vertical greenery species (*H. helix*). Specifically, the influence of three moss species on surface temperature, near-surface air temperature, and the temperature of the underlying substrate material was assessed under different typical weather conditions and compared to both bare mortar and samples covered with *H. helix*. Based on the findings, the following conclusions were drawn:

- Due to their low albedo, moss responds strongly to direct sunlight, resulting in increased surface temperatures under sunny conditions. This resulted in average daytime surface temperatures that were $1.6 \text{ }^{\circ}\text{C}$ to $4.2 \text{ }^{\circ}\text{C}$ higher than those of bare mortar during hot and sunny weather, with average peak temperature differences between $8.3 \text{ }^{\circ}\text{C}$ and $19.2 \text{ }^{\circ}\text{C}$ higher. This heating effect was more pronounced in acrocarp moss species (*G. pulvinata* and *P. capillare*) than in the pleurocarp species (*B. rutabulum*).
- Moss exhibits insulating properties, reducing the amplitude of daily temperature fluctuations inside the bioreceptive mortar base layer. While average peak daytime temperatures inside the underlying mortar were reduced by up to $2.6 \text{ }^{\circ}\text{C}$, the overall internal temperature—both day and night—was on average $0.3 \text{ }^{\circ}\text{C}$ to $2.8 \text{ }^{\circ}\text{C}$ higher, as heat was released slowly. However, a substantial portion of these insulating properties is lost when surface coverage is incomplete. Moss has no significant effect on air temperatures in the near-surface boundary layer during cold and/or cloudy weather, but during hot and sunny conditions, moss, and specifically *B. rutabulum*, significantly increases the near-surface air temperatures both during the day and the night, although the overall effect on urban air temperatures at a larger scale remains tentative.
- Watering moss temporarily reduces air and surface temperatures, but the effect only has a short duration, whereas it reduces the insulating properties of the moss at the same time.
- The climbing plant *H. helix* recorded average daytime and nighttime air, surface, and material temperatures similar to, or lower than, those of moss under all tested weather conditions. This effect is primarily associated with surface shading, as *H. helix* showed no sign of insulating properties.

Overall, the results suggest that applying moss to vertical structures could be overall beneficial in colder climates, but requires careful consideration if heat stress is a concern. The primary thermal benefit of

moss lies in its insulating properties, which can buffer the temperature difference between the interior and exterior. This could lead to energy savings when used on buildings with interior climate control, although the extent of this effect is dependent on the moisture levels in the moss. On the other hand, when moss is applied to surfaces subjected to direct sunlight, its effects on the local thermal climate and interior temperatures can be deleterious – depending also on the thermal properties of the original surface material - due to an increase in surface temperature leading to increased near-surface air temperatures and mean radiant temperature, as well as an increase in the temperature of the substrate material. Although this may be beneficial during colder seasons or climates, the effect is strongest in summer, when sunlight intensity is at its highest. As such, moss application may contribute to the Urban Heat Island and thermal stress experienced by humans through increased air and radiant temperatures, although this effect will have to be verified at a larger scale. This effect can be partially mitigated by keeping the moss hydrated, careful species selection, or shading the moss, either artificially or naturally. This last option may be the most effective, as it combines the shading properties of vascular plants with the acoustic absorption, particulate matter capture, and thermal insulation provided by moss. However, further research is necessary to validate these findings in larger spatial and temporal scales and under more varying weather conditions. Furthermore, future research could also focus on optimising shading strategies and assessing the moss's effect on indoor temperatures under varying weather conditions and interior heat-load scenarios.

CRedit authorship contribution statement

M. Veeger: Writing – review & editing, Visualization, Validation, Software, Methodology, Investigation, Formal analysis, Data curation, Conceptualization. **M. Ottele:** Writing – review & editing, Supervision, Methodology, Conceptualization. **H.M. Jonkers:** Writing – review & editing, Supervision, Methodology, Funding acquisition, Conceptualization.

Funding

This work was supported by the NWO Hidden Biodiversity project, file number NWA.1389.20.111.

Declaration of competing interest

The authors declare the following financial interests/personal relationships which may be considered as potential competing interests: M. Veeger reports a relationship with ReSpyre B.V. that includes: consulting or advisory.

M. Ottele reports a relationship with ReSpyre B.V. that includes: equity or stocks.

H.M. Jonkers reports a relationship with ReSpyre B.V. that includes: equity or stocks.

If there are other authors, they declare that they have no known competing financial interests or personal relationships that could have appeared to influence the work reported in this paper.

Acknowledgements

We want to thank the Hortus Botanicus Delft for graciously hosting our experiment.

Appendix A. Supplementary data

Supplementary data to this article can be found online at <https://doi.org/10.1016/j.scitotenv.2026.181830>.

Data availability

The full dataset, sensor designs and schematics, and code used are available on Mendeley Data under the following DOI: <https://doi.org/10.17632/fb2z9gfd2.1>

References

- Allen, R., Tasumi, M., Trezza, R., Waters, R., Bastiaanssen, W., 2002. SEBAL (surface energy balance algorithms for land). Advance training and users manual-Idaho implementation version, vol. 1, 97.
- L. M. Al-Saadi, S. H. Jaber, and M. H. Al-Jiboori, "Variation of urban vegetation cover and its impact on minimum and maximum heat islands," *Urban Clim.*, vol. 34, p. 100707, 2020/12/01/ 2020, doi:<https://doi.org/10.1016/j.uclim.2020.100707>.
- A. K. M. Amir, Y. Katoh, H. Katsurayama, M. Koganei, and M. Mizunuma, "Effects of convection heat transfer on Sunagoke moss green roof: a laboratory study," *Energ. Buildings*, vol. 158, pp. 1417–1428, 2018/01/01/ 2018, doi:<https://doi.org/10.1016/j.enbuild.2017.11.043>.
- T. Asaeda, V. T. Ca, and A. Wake, "Heat storage of pavement and its effect on the lower atmosphere," *Atmos. Environ.*, vol. 30, no. 3, pp. 413–427, 1996/02/01/ 1996, doi:[https://doi.org/10.1016/1352-2310\(94\)00140-5](https://doi.org/10.1016/1352-2310(94)00140-5).
- Z. Azkorra-Larrinaga, A. Erkoreka-González, K. Martín-Escudero, E. Pérez-Iribarren, and N. Romero-Antón, "Thermal characterization of a modular living wall for improved energy performance in buildings," *Build. Environ.*, vol. 234, p. 110102, 2023/04/15/ 2023, doi:<https://doi.org/10.1016/j.buildenv.2023.110102>.
- R. Bakhshoodeh, C. Ocampo, and C. Oldham, "Exploring the evapotranspirative cooling effect of a green façade," *Sustain. Cities Soc.*, vol. 81, p. 103822, 2022/06/01/ 2022, doi:<https://doi.org/10.1016/j.scs.2022.103822>.
- W. Block, R. I. Lewis Smith, and A. D. Kennedy, "Strategies of survival and resource exploitation in the Antarctic fellfield ecosystem," *Biol. Rev.*, vol. 84, no. 3, pp. 449–484, 2009/08/01 2009, doi:<https://doi.org/10.1111/j.1469-185X.2009.00084.x>.
- D. Blok et al., "The cooling capacity of mosses: controls on water and energy fluxes in a Siberian tundra site," *Ecosystems*, vol. 14, no. 7, pp. 1055–1065, 2011/11/01 2011, doi:<https://doi.org/10.1007/s10021-011-9463-5>.
- B. Bond-Lamberty, S. T. Gower, B. Amiro, and B. E. Ewers, "Measurement and modelling of bryophyte evaporation in a boreal forest chronosequence," *Ecology*, vol. 4, no. 1, pp. 26–35, 2011/01/01 2011, doi:<https://doi.org/10.1002/eco.118>.
- A. Y. Davis, J. Jung, B. C. Pijanowski, and E. S. Minor, "Combined vegetation volume and "greenness" affect urban air temperature," *Appl. Geogr.*, vol. 71, pp. 106–114, 2016/06/01/ 2016, doi:<https://doi.org/10.1016/j.apgeog.2016.04.010>.
- J. M. A. Duncan, B. Boruff, A. Saunders, Q. Sun, J. Hurlley, and M. Amati, "Turning down the heat: an enhanced understanding of the relationship between urban vegetation and surface temperature at the city scale," *Sci. Total Environ.*, vol. 656, pp. 118–128, 2019/03/15/ 2019, doi:<https://doi.org/10.1016/j.scitotenv.2018.11.223>.
- Ebi, K.L., et al., 2021. Hot weather and heat extremes: health risks. *Lancet* 398 (10301), 698–708. [https://doi.org/10.1016/S0140-6736\(21\)01208-3](https://doi.org/10.1016/S0140-6736(21)01208-3).
- J. L. Edmondson, I. Stott, Z. G. Davies, K. J. Gaston, and J. R. Leake, "Soil surface temperatures reveal moderation of the urban heat island effect by trees and shrubs," *Sci. Rep.*, vol. 6, no. 1, p. 33708, 2016/09/19 2016, doi:<https://doi.org/10.1038/sr33708>.
- G. L. Feyisa, K. Dons, and H. Meilby, "Efficiency of parks in mitigating urban heat island effect: an example from Addis Ababa," *Landscape Urban Plan.*, vol. 123, pp. 87–95, 2014/03/01/ 2014, doi:<https://doi.org/10.1016/j.landurbplan.2013.12.008>.
- K. P. Gallo, A. L. McNab, T. R. Karl, J. F. Brown, J. J. Hood, and J. D. Tarpley, "The use of a vegetation index for assessment of the urban heat island effect," *Int. J. Remote Sens.*, vol. 14, no. 11, pp. 2223–2230, 1993/07/01 1993, doi:<https://doi.org/10.1080/01431169308954031>.
- Gimingham, C.H., Smith, R.L.L., 1971. Growth form and water relations of mosses in the maritime Antarctic. *Br. Antarct. Survey Bull.* 25, 1–21 [Online]. Available: <https://nora.nerc.ac.uk/id/eprint/526460>.
- J. L. Gornall, I. S. Jónsdóttir, S. J. Woodin, and R. Van der Wal, "Arctic mosses govern below-ground environment and ecosystem processes," *Oecologia*, vol. 153, no. 4, pp. 931–941, 2007/10/01 2007, doi:<https://doi.org/10.1007/s00442-007-0785-0>.
- Havenith, G., Fiala, D., 2015. "thermal indices and Thermophysiological modeling for heat stress," in *comprehensive. Physiology* 255–302.
- Haynes, A., Popek, R., Boles, M., Paton-Walsh, C., Robinson, S.A., 2019. Roadside Moss turfs in south East Australia capture more particulate matter along an urban gradient than a common native tree species. *Atmosphere* 10 (4). <https://doi.org/10.3390/atmos10040224>.
- C. Heaviside, H. Macintyre, and S. Vardoulakis, "the urban Heat Island: implications for health in a changing environment," *current environmental Health Rep.*, vol. 4, no. 3, pp. 296–305, 2017/09/01 2017, doi:<https://doi.org/10.1007/s40572-017-0150-3>.
- L. D. Hinzman, D. L. Kane, R. E. Gieck, and K. R. Everett, "Hydrologic and thermal properties of the active layer in the Alaskan Arctic," *Cold Reg. Sci. Technol.*, vol. 19, no. 2, pp. 95–110, 1991/05/01/ 1991, doi:[https://doi.org/10.1016/0165-232X\(91\)90001-W](https://doi.org/10.1016/0165-232X(91)90001-W).
- M. Hou, Y. Hu, and Y. He, "Modifications in vegetation cover and surface albedo during rapid urbanization: a case study from South China," *Environ. Earth Sci.*, vol. 72, no. 5, pp. 1659–1666, 2014/09/01 2014, doi:<https://doi.org/10.1007/s12665-014-3070-7>.
- W. T. K. Huang et al., "economic valuation of temperature-related mortality attributed to urban heat islands in European cities," *nature Communications*, vol. 14, no. 1, p. 7438, 2023/11/17 2023, doi:<https://doi.org/10.1038/s41467-023-43135-z>.

- K. Ip, M. Lam, and A. Miller, "Shading performance of a vertical deciduous climbing plant canopy," *Build. Environ.*, vol. 45, no. 1, pp. 81–88, 2010/01/01/ 2010, doi:<https://doi.org/10.1016/j.buildenv.2009.05.003>.
- IPCC, 2023a. "Current Status and Trends," *Climate Change 2023: Synthesis report*. In: Team, C.W., Lee, H., Romero, J. (Eds.), Contribution of working groups I, II and III to the sixth assessment report of the intergovernmental panel on climate change. IPCC, Geneva, Switzerland, pp. 41–66.
- IPCC, 2023b. "Long-Term Climate and Development Futures," *Climate Change 2023: Synthesis report*. In: Team, C.W., Lee, H., Romero, J. (Eds.), Contribution of working groups I, II and III to the sixth assessment report of the intergovernmental panel on climate change. IPCC, Geneva, Switzerland, pp. 67–90.
- M. Jin, R. E. Dickinson, and D. Zhang, "the footprint of urban areas on global climate as characterized by MODIS," (in English), *J. Clim.*, vol. 18, no. 10, pp. 1551–1565, 15 May. 2005 2005, doi:<https://doi.org/10.1175/JCLI3334.1>.
- C. Jongsoo and L. Jeasun, "Evaluation of the temperature-reduction effects of moss-based green roofs," *Energ. Buildings*, vol. 352, p. 116835, 2026/02/01/ 2026, doi:<https://doi.org/10.1016/j.enbuild.2025.116835>.
- K. J. Kontoleon and E. A. Eumorfopoulou, "The effect of the orientation and proportion of a plant-covered wall layer on the thermal performance of a building zone," *Build. Environ.*, vol. 45, no. 5, pp. 1287–1303, 2010/05/01/ 2010, doi:<https://doi.org/10.1016/j.buildenv.2009.11.013>.
- M. Koranda and A. Michelsen, "Mosses reduce soil nitrogen availability in a subarctic birch forest via effects on soil thermal regime and sequestration of deposited nitrogen," *J. Ecol.*, vol. 109, no. 3, pp. 1424–1438, 2021/03/01 2021, doi:<https://doi.org/10.1111/1365-2745.13567>.
- D. Kumar and S. Shekhar, "Statistical analysis of land surface temperature-vegetation indexes relationship through thermal remote sensing," *Ecotoxicol. Environ. Saf.*, vol. 121, pp. 39–44, 2015/11/01/ 2015, doi:<https://doi.org/10.1016/j.ecoenv.2015.07.004>.
- H. Kusaka and F. Kimura, "thermal effects of urban canyon structure on the nocturnal Heat Island: numerical experiment using a mesoscale model coupled with an urban canopy model," (in English), *J. Appl. Meteorol.*, vol. 43, no. 12, pp. 1899–1910, 01 Dec. 2004 2004, doi:<https://doi.org/10.1175/JAM2169.1>.
- S. Li and B. Xiao, "Cyanobacteria and moss biocrusts increase evaporation by regulating surface soil moisture and temperature on the northern loess plateau, China," *CATENA*, vol. 212, p. 106068, 2022/05/01/ 2022, doi:<https://doi.org/10.1016/j.catena.2022.106068>.
- J. Liu et al., "Is there an association between hot weather and poor mental health outcomes? A systematic review and meta-analysis," *Environ. Int.*, vol. 153, p. 106533, 2021/08/01/ 2021, doi:<https://doi.org/10.1016/j.envint.2021.106533>.
- Liu, J., et al., 2022. Heat exposure and cardiovascular health outcomes: a systematic review and meta-analysis. *Lancet Planet. Health* 6 (6), e484–e495. [https://doi.org/10.1016/S2542-5196\(22\)00117-6](https://doi.org/10.1016/S2542-5196(22)00117-6).
- L.-c. Liu, S.-z. Li, Z.-h. Duan, T. Wang, Z.-s. Zhang, and X.-r. Li, "Effects of microbiotic crusts on dew deposition in the restored vegetation area at Shapotou, Northwest China," *J. Hydrol.*, vol. 328, no. 1, pp. 331–337, 2006/08/30/ 2006, doi:<https://doi.org/10.1016/j.jhydrol.2005.12.004>.
- L. Mentaschi et al., "Global long-term mapping of surface temperature shows intensified intra-city urban heat island extremes," *Glob. Environ. Chang.*, vol. 72, p. 102441, 2022/01/01/ 2022, doi:<https://doi.org/10.1016/j.gloenvcha.2021.102441>.
- A. A. Millward, M. Torchia, A. E. Laursen, and L. D. Rothman, "Vegetation placement for summer built surface temperature moderation in an urban microclimate," *Environ. Manag.*, vol. 53, no. 6, pp. 1043–1057, 2014/06/01 2014, doi:<https://doi.org/10.1007/s00267-014-0260-8>.
- P. J. M. Monteiro, S. A. Miller, and A. Horvath, "Towards sustainable concrete," *Nat. Mater.*, vol. 16, no. 7, pp. 698–699, 2017/07/01 2017, doi:<https://doi.org/10.1038/nmat4930>.
- Nunez, M., Oke, T.R., 01 Jan. 1977. "The Energy Balance of an Urban Canyon," (in English). *J. Appl. Meteorol. Climatol.* 16 (1), 11–19. [https://doi.org/10.1175/1520-0450\(1977\)016<0011:TEBOAU>2.0.CO;2](https://doi.org/10.1175/1520-0450(1977)016<0011:TEBOAU>2.0.CO;2), 1977.
- O'Donnell, J.A., Romanovsky, V.E., Harden, J.W., McGuire, A.D., 2009a. The Effect of Moisture Content on the Thermal Conductivity of Moss and Organic Soil Horizons From Black Spruce Ecosystems in Interior Alaska. *Soil Sci. 174* (12) [Online]. Available: https://journals.lww.com/soilsci/fulltext/2009/12000/the_effect_of_moisture_content_on_the_thermal.2.aspx.
- O'Donnell, J.A., Romanovsky, V.E., Harden, J.W., McGuire, A.D., 2009b. The effect of moisture content on the thermal conductivity of Moss and Organic soil horizons from Black Spruce ecosystems in interior Alaska. *Soil Sci. 174* (12), 646–651. <https://doi.org/10.1097/SS.0b013e3181c4a7f8>.
- R. O'Hegarty, G. Amedeo, and O. Kinnane, "The impact of compromised insulation on building energy performance," *Energ. Buildings*, vol. 316, p. 114337, 2024/08/01/ 2024, doi:<https://doi.org/10.1016/j.enbuild.2024.114337>.
- Oke, T.R., 1987. *Boundary Layer Climates*, 2nd ed. Routledge.
- T. R. Oke, G. T. Johnson, D. G. Steyn, and I. D. Watson, "Simulation of surface urban heat islands under 'ideal' conditions at night part 2: diagnosis of causation," *Bound.-Layer Meteorol.*, vol. 56, no. 4, pp. 339–358, 1991/09/01 1991, doi:<https://doi.org/10.1007/BF00119211>.
- A. Ossola, G. D. Jenerette, A. McGrath, W. Chow, L. Hughes, and M. R. Leishman, "Small vegetated patches greatly reduce urban surface temperature during a summer heatwave in Adelaide, Australia," *Landsc. Urban Plan.*, vol. 209, p. 104046, 2021/05/01/ 2021, doi:<https://doi.org/10.1016/j.landurbplan.2021.104046>.
- G. Pérez, L. Rincón, A. Vila, J. M. González, and L. F. Cabeza, "Green vertical systems for buildings as passive systems for energy savings," *Appl. Energy*, vol. 88, no. 12, pp. 4854–4859, 2011/12/01/ 2011, doi:<https://doi.org/10.1016/j.apenergy.2011.06.032>.
- L. Pérez-Urrestarazu, "Water consumption of felt-based outdoor living walls in warm climates," *Urban For. Urban Green.*, vol. 59, p. 127025, 2021/04/01/ 2021, doi:<https://doi.org/10.1016/j.ufug.2021.127025>.
- K. Perini, P. Castellari, M. Calbi, S. Prandi, and E. Roccitiello, "Fine dust collection capacity of a moss greening system for the building envelope: an experimental approach," *Build. Environ.*, vol. 267, p. 112203, 2025/01/01/ 2025, doi:<https://doi.org/10.1016/j.buildenv.2024.112203>.
- K. Perini, P. Castellari, D. Gisotti, A. Giachetta, C. Turcato, and E. Roccitiello, "MosSkin: a moss-based lightweight building system," *Build. Environ.*, vol. 221, p. 109283, 2022/08/01/ 2022, doi:<https://doi.org/10.1016/j.buildenv.2022.109283>.
- D. E. Petzold and A. N. Rencz, "The albedo of selected subarctic surfaces," *Arct. Alp. Res.*, vol. 7, no. 4, pp. 393–398, 1975/11/01 1975, doi:<https://doi.org/10.1080/00040851.1975.12003850>.
- PMCMRplus: Calculate Pairwise Multiple Comparisons of Mean Rank Sums Extended, 2024.
- R Core Team, 2023. *R: A Language and Environment for Statistical Computing*, ed. R Foundation for Statistical Computing, Vienna, Austria.
- P. Shafiq, I. Asadi, A. R. Akhiani, N. B. Mahyuddin, and M. Hashemi, "Thermal properties of cement mortar with different mix proportions," *Mater. Constr.*, vol. 70, no. 339, p. e224, 09/15 2020, doi:<https://doi.org/10.3989/mc.2020.09219>.
- Sharratt, B.S., 1997. Thermal conductivity and water retention of a BLACK SPRUCE forest floor. *Soil Sci.* 162 (8) [Online]. Available: https://journals.lww.com/soilsci/fulltext/1997/08000/thermal_conductivity_and_water_retention_of_a.6.aspx.
- N. A. Soudzilovskaia, P. M. van Bodegom, and J. H. C. Cornelissen, "Dominant bryophyte control over high-latitude soil temperature fluctuations predicted by heat transfer traits, field moisture regime and laws of thermal insulation," *Funct. Ecol.*, vol. 27, no. 6, pp. 1442–1454, 2013/12/01 2013, doi:<https://doi.org/10.1111/1365-2435.12127>.
- E. Stache, B. Schilperoot, M. Ottlé, and H. M. Jonkers, "Comparative analysis in thermal behaviour of common urban building materials and vegetation and consequences for urban heat island effect," *Build. Environ.*, vol. 213, p. 108489, 2022/04/01/ 2022, doi:<https://doi.org/10.1016/j.buildenv.2021.108489>.
- L. Stohl, T. Manninger, J. von Werder, F. Dehn, A. Gorbushina, and B. Meng, "Bioreceptivity of concrete: a review," *J. Build. Eng.*, vol. 76, p. 107201, 2023/10/01/ 2023, doi:<https://doi.org/10.1016/j.job.2023.107201>.
- P. C. Stoy, L. E. Street, A. V. Johnson, A. Prieto-Blanco, and S. A. Ewing, "Temperature, heat flux, and reflectance of common subarctic mosses and lichens under field conditions: might changes to community composition impact climate-relevant surface fluxes?," *Arct. Antarct. Alp. Res.*, vol. 44, no. 4, pp. 500–508, 2012/11/01 2012, doi:<https://doi.org/10.1657/1938-4246-44.4.500>.
- T. Susca, S. R. Gaffin, and G. R. Dell'Osso, "Positive effects of vegetation: urban heat island and green roofs," *Environ. Pollut.*, vol. 159, no. 8, pp. 2119–2126, 2011/08/01/ 2011, doi:<https://doi.org/10.1016/j.envpol.2011.03.007>.
- H. Taha, "Urban climates and heat islands: albedo, evapotranspiration, and anthropogenic heat," *Energ. Buildings*, vol. 25, no. 2, pp. 99–103, 1997/01/01/ 1997, doi:[https://doi.org/10.1016/S0378-7788\(96\)00999-1](https://doi.org/10.1016/S0378-7788(96)00999-1).
- H. Takebayashi and M. Moriyama, "Study on surface heat budget of various pavements for urban Heat Island mitigation," *Adv. Mater. Sci. Eng.*, vol. 2012, no. 1, p. 523051, 2012/01/01 2012, doi:<https://doi.org/10.1155/2012/523051>.
- Tamamkani Eshfehankalateh, A., Ngarambe, J., Yun, G.Y., 2021. Influence of tree canopy coverage and leaf area density on urban heat island mitigation. *Sustainability* 13 (13). <https://doi.org/10.3390/su13137496>.
- A. Trlica, L. R. Hutryra, C. L. Schaaf, A. Erb, and J. A. Wang, "albedo, land cover, and daytime surface temperature variation across an urbanized landscape," *earth's Future*, vol. 5, no. 11, pp. 1084–1101, 2017/11/01 2017, doi:<https://doi.org/10.1002/2017EF000569>.
- Veeger, M., Ottlé, M., Jonkers, H.M., 2025a. Evaluating mosses on bioreceptive concrete: effective sound absorbers? *Build. Environ.* 281, 113194. <https://doi.org/10.1016/j.buildenv.2025.113194>.
- Veeger, M., Ottlé, M., Jonkers, H.M., 2026. Growing moss on bioreceptive concrete using a novel two-step approach: the effects of light, water, and species selection. *Ecol. Eng.* 223, 107839. <https://doi.org/10.1016/j.ecoleng.2025.107839>.
- Veeger, M., Ottlé, M., Prieto, A., 2021. Making bioreceptive concrete: formulation and testing of bioreceptive concrete mixtures. *J. Build. Eng.* 44, 102545. <https://doi.org/10.1016/j.job.2021.102545>.
- Veeger, M., Veenendaal, E.M., Limpens, J., Ottlé, M., Jonkers, H.M., 2025b. Moss species for bioreceptive concrete: a survey of epilithic urban moss communities and their dynamics. *Ecol. Eng.* 212, 107502. <https://doi.org/10.1016/j.ecoleng.2024.107502>.
- Wang, Y., Zhang, Y., Ding, N., Qin, K., Yang, X., 2020. Simulating the impact of urban surface evapotranspiration on the urban heat island effect using the modified RS-PM model: a case study of Xuzhou, China. *Remote Sens.* 12 (3). <https://doi.org/10.3390/rs12030578>.
- Q. Weng, D. Lu, and J. Schubring, "Estimation of land surface temperature-vegetation abundance relationship for urban heat island studies," *Remote Sens. Environ.*, vol. 89, no. 4, pp. 467–483, 2004/02/29/ 2004, doi:<https://doi.org/10.1016/j.rse.2003.11.005>.
- S. N. Williamson, I. C. Barrio, D. S. Hik, and J. A. Gamon, "Phenology and species determine growing-season albedo increase at the altitudinal limit of shrub growth in the sub-Arctic," *Glob. Chang. Biol.*, vol. 22, no. 11, pp. 3621–3631, 2016/11/01 2016, doi:<https://doi.org/10.1111/gcb.13297>.
- B. Xiao and M. A. Bowker, "Moss-biocrusts strongly decrease soil surface albedo, altering land-surface energy balance in a dryland ecosystem," *Sci. Total Environ.*, vol. 741, p. 140425, 2020/11/01/ 2020, doi:<https://doi.org/10.1016/j.scitotenv.2020.140425>.
- B. Xiao, K. Hu, T. Ren, and B. Li, "Moss-dominated biological soil crusts significantly influence soil moisture and temperature regimes in semiarid ecosystems," *Geoderma*,

- vol. 263, pp. 35–46, 2016/02/01/ 2016, doi:<https://doi.org/10.1016/j.geoderma.2015.09.012>.
- B. Xiao, S. Ma, and K. Hu, "Moss biocrusts regulate surface soil thermal properties and generate buffering effects on soil temperature dynamics in dryland ecosystem," *Geoderma*, vol. 351, pp. 9–24, 2019/10/01/ 2019, doi:<https://doi.org/10.1016/j.geoderma.2019.05.017>.
- C. Yan, Q. Guo, H. Li, L. Li, and G. Y. Qiu, "Quantifying the cooling effect of urban vegetation by mobile traverse method: a local-scale urban heat island study in a subtropical megacity," *Build. Environ.*, vol. 169, p. 106541, 2020/02/01/ 2020, doi:<https://doi.org/10.1016/j.buildenv.2019.106541>.
- J. Zhang, Y.-m. Zhang, A. Downing, J.-h. Cheng, X.-b. Zhou, and B.-c. Zhang, "The influence of biological soil crusts on dew deposition in Gurbantunggut Desert, northwestern China," *J. Hydrol.*, vol. 379, no. 3, pp. 220–228, 2009/12/30/ 2009, doi:<https://doi.org/10.1016/j.jhydrol.2009.09.053>.
- Y. Zhang, C. Yu, and L. Wang, "Temperature exposure during pregnancy and birth outcomes: an updated systematic review of epidemiological evidence," *Environ. Pollut.*, vol. 225, pp. 700–712, 2017/06/01/ 2017, doi:<https://doi.org/10.1016/j.envpol.2017.02.066>.
- J. Zhao *et al.*, "Assessing the thermal contributions of urban land cover types," *Landsc. Urban Plan.*, vol. 204, p. 103927, 2020/12/01/ 2020, doi:<https://doi.org/10.1016/j.landurbplan.2020.103927>.